Dyke–brittle shear relationships in the Western Deccan Strike-slip Zone around Mumbai (Maharashtra, India)

ACHYUTA AYAN MISRA[1]* & SOUMYAJIT MUKHERJEE[2]

[1]*Exploration, Reliance Industries Ltd., Mumbai 400 701, Maharashtra, India*

[2]*Department of Earth Sciences, Indian Institute of Technology Bombay, Mumbai 400 076, Maharashtra, India*

**Correspondence: achyutaayan@gmail.com*

Abstract: Dykes are abundant in the Deccan Large Igneous Province, and those to the west are referred to as the 'coastal swarm'. Most of the coastal swarm dykes appear in the Western Deccan Strike-slip Zone (WDSZ). Faults with N–S, NE–SW and NW–SE trends (brittle shears) have been reported in the WDSZ around Mumbai. However, details of their relationships with Deccan dykes, which can easily be studied at sub-horizontal outcrops, have remained unknown. Previous authors have classified dykes in the WDSZ according to their isotopic ages as group I (*c.* 65.6 Ma), group II (*c.* 65 Ma) and group III (64–63 Ma). Dykes have also been categorized on the basis of field observations; group I dykes were found to pre-date deformation related to the separation of Seychelles and India, whereas group II and III dykes post-date this event. Our field studies reveal group I dykes to be faulted/sheared and lacking a uniform trend, whereas group II and III dykes have approximately N–S, NW–SE and NE–SW trends and intrude brittle shears/fault planes. We have also found evidence of syn-deformation intrusion in the group II and III dykes: e.g. P-planes along the dyke margins and grooves in the baked zone of dykes. These two groups of dykes match the trends of dominantly sinistral brittle shears. Of the 43 dykes studied, only ten belong to group I, and we conclude that a large proportion of the dykes in the WDSZ belong to groups II and III. It is erroneous to interpret the Seychelles–India rifting as simple near-E–W extension at *c.* 63–62 Ma from the general approximately N–S trend of the dykes; the direction of brittle extension must instead be deduced from brittle shears/fault planes.

Supplementary material: Stereo plots and reduced stress tensors for all faults and brittle shears are available at https://doi.org/10.6084/m9.figshare.c.3259627

Dykes provide several classes of tectonomagmatic information (e.g. Hanski *et al.* 2006; Paquet *et al.* 2007; reviews by Gudmundsson 2011; Srivastava 2011), and may even be used to reconstruct the local palaeostresses during their emplacement (e.g. Martínez-Poza *et al.* 2014). They have also been used to map regional stress patterns and their variations (Glazner *et al.* 1999 and references therein; Mège & Korme 2004), and have been studied in detail using field mapping and analogue/numerical modelling (e.g. Gaffney *et al.* 2007; Kavanagh & Sparks 2011 and references therein; Abdelmalak *et al.* 2012; Hodge *et al.* 2012; Xu *et al.* 2013). Two processes for dyking are acknowledged: (i) intrusion into massive or undeformed host rock, and (ii) filling of pre-existing fractures/anisotropies (Xu *et al.* 2013; Fig. 1a). The tensile strength of pre-existing structures such as faults or foliation is usually negligible (see reviews by Misra & Mukherjee 2015*a*), and in most cases rocks naturally possess pre-existing structures or anisotropies. Therefore, intrusions are generally mixed mode.

In a homogenous isotropic medium, dykes are generally emplaced perpendicular to the direction of regional extension (σ_3) (Fig. 1b) (Anderson 1951). The length and thickness of dykes are controlled by fluid overpressure in the magma chamber (e.g. Ray *et al.* 2007). Thus, in pure dilation, there is no shear stress parallel to the dyke trend, and opening will usually occur only perpendicular to the margins (mode I fracturing). However, reducing dyke intrusion to such emplacement mechanics is simplistic and does not explain all observations; dykes may also be associated with host rock brecciation, stoping and magma solidification, or may be emplaced in a strike-slip setting (Hutton 1992; Glazner *et al.* 1999; Correa-Gomes *et al.* 2001; Aubourg *et al.* 2002; Valentine & Krogh 2006; Kavanagh & Sparks 2011; Rivalta *et al.* 2015). In a strike-slip setting, a hybrid fracturing mode is dominant.

Dyke trends may not always indicate simple regional stress fields, e.g. when dykes intrude pre-existing fractures and faults, opening may be oblique to their margins (Glazner *et al.* 1999 and

From: Mukherjee, S., Misra, A. A., Calvès, G. & Nemčok, M. (eds) 2017. *Tectonics of the Deccan Large Igneous Province*. Geological Society, London, Special Publications, **445**, 269–295.
First published online June 22, 2016, https://doi.org/10.1144/SP445.4

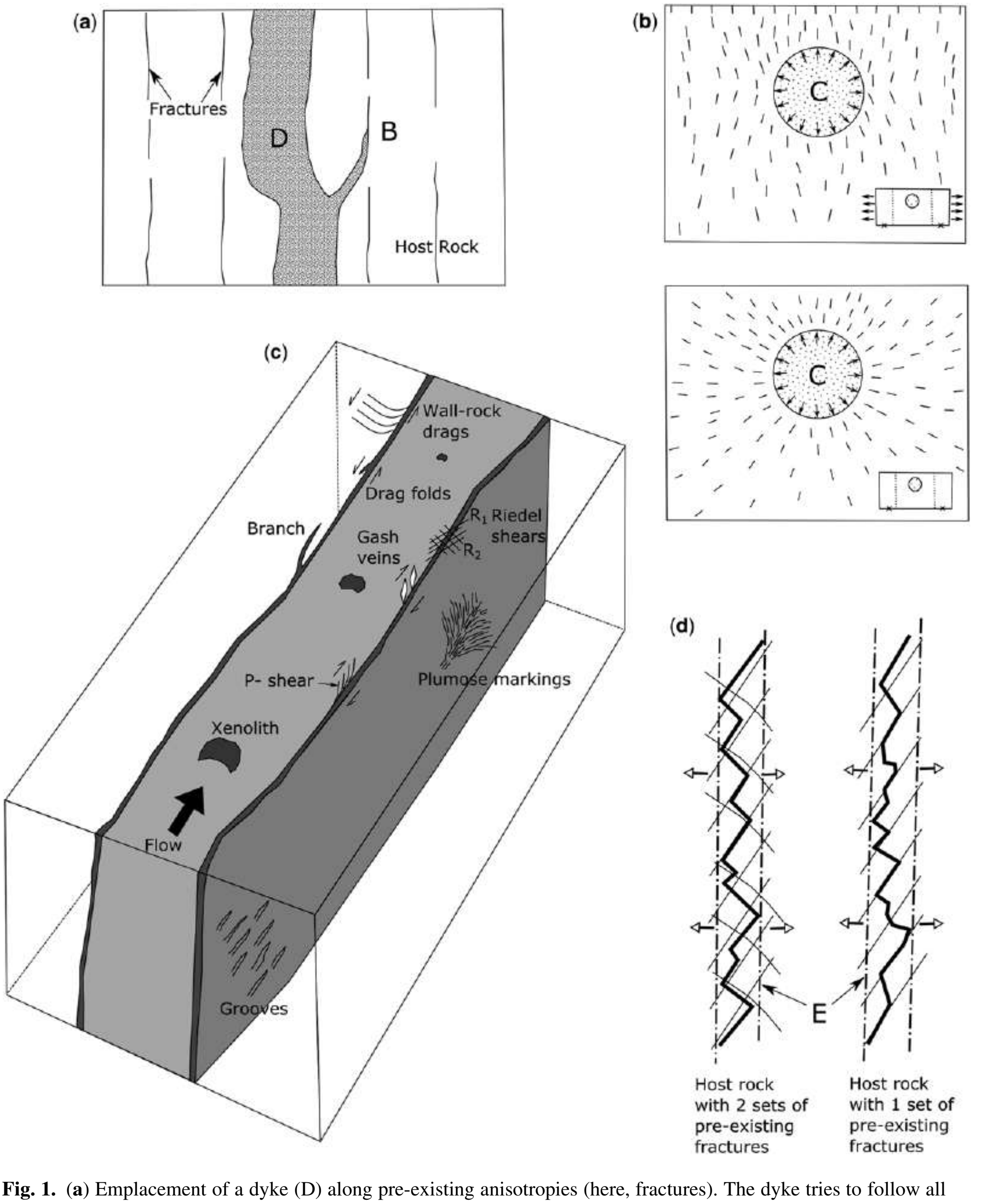

Fig. 1. (**a**) Emplacement of a dyke (D) along pre-existing anisotropies (here, fractures). The dyke tries to follow all the fractures in its proximity but chooses the weakest, i.e. the one with the least tensile strength. The dyke also attempts to follow another fracture and branch (B) off the main dyke (modified from Gudmundsson 1984, fig. 1). (**b**) Vertical section showing stress trajectories within an isotropic homogeneous rock near a circular magma chamber (C). Upper: magmatic stresses in the presence of horizontal extension; lower: only magmatic stress. The tick marks denote σ_1 axes. Dykes will be emplaced along these axes. Note that in the absence of extension, dyke dips are expected to become gentler progressively away from the magma chamber (modified from Gudmundsson 2002, figs 3 & 4). (**c**) Structures observed in syn-deformation or post-deformation intrusion (modified from Correa-Gomes *et al.* 2001, fig. 11). Not all structures shown here are observed in this study, and those observed are P-shears, wall-rock drag, grooves and branches. (**d**) Dykes emplaced in two sets (left) and one set (right) of pre-existing anisotropies (here, fractures). Blank arrows: extension direction; dotted line marked E: dyke envelope (modified from Hoek 1991, fig. 6). Examples of this can be seen in Figure 9a and c.

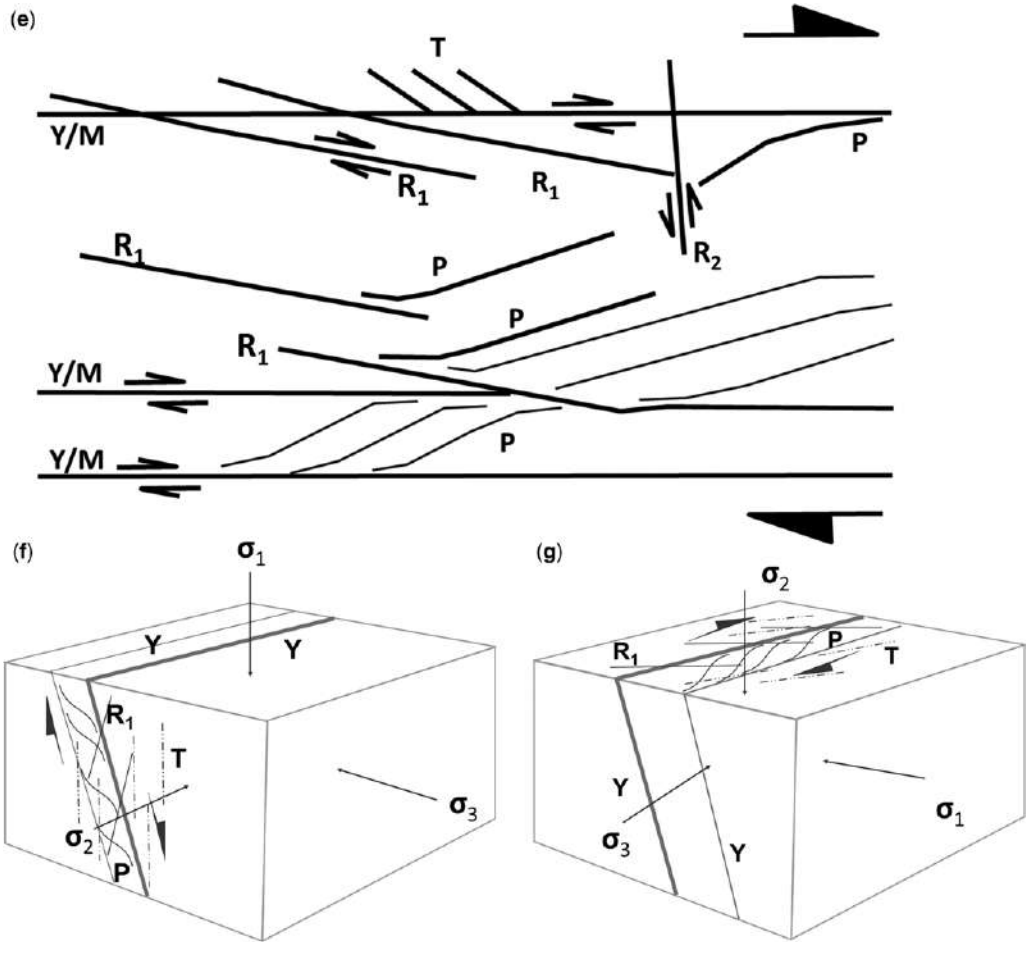

Fig. 1. (*Continued*) (**e**) Schematic diagram showing the different types of fractures/shears occurring in a brittle shear zone (Y- and P-planes) and Riedel shear system (R_1, R_2, P, T and M fractures). The stress orientations implicated by the shears are also shown in the diagram (modified from Passchier & Trouw 2005). R, Riedel shears; P, shear fractures; T, extension fractures; M, average slip surface (fault). Block diagrams showing brittle shears in case of (**f**) a normal fault and (**g**) a strike-slip fault with the related stress regime.

references therein; Perry *et al.* 2006; Valentine & Keating 2007). Although dykes of type (i) described above form normal to σ_3, they may not always be pure extensional fractures (Mériaux & Lister 2002). In the absence of far-field tensile stresses, dykes originating from deep magma chambers are expected to be radial, as opposed to parallel, for pure extensional fractures, and may extend up to tens of kilometres (Gudmundsson 2002, fig. 4). The model in Figure 1b predicts only a few subvertical dykes at shallow crustal depth, but moving away from directly above the magma chamber the dyke dip decreases. Another possibility is the formation of cone-sheets, i.e. inward-dipping sheet-like intrusions that are not radial (e.g. Galland *et al.* 2014). When far-field tensile stresses prevail, e.g. in rift zones, almost all dykes are subvertical (Fig. 1b). When dykes are emplaced, the local compression axes (σ_1) temporarily maintain a high angle or are perpendicular to the dyke (Gudmundsson 2011, fig. 2.13). The dykes perturb the stress field and increase local horizontal stress that may temporarily exceed the far-field maximum vertical stress (σ_1). Thus, newer dykes in a rift zone can be emplaced only after compressive stresses are reduced by interaction with other far-field stresses. Therefore, if dykes are cross-cutting, this indicates that they were emplaced during two different phases separated by time periods ranging from a few days (Gudmundsson 1984) to a few million years (Hooper *et al.* 2010). This applies for type (i) and (ii) dykes mentioned above, since local σ_1 axes are always perpendicular to the dyke trend. Conjugate cross-cutting dykes are rare (Srivastava 2011). Dykes may be emplaced during numerous phases of short temporal span (e.g. Heaman & Tarney 1989; Bleeker & Ernst 2006; Hooper *et al.* 2010), and each such phase induces tensile stress in the crust (Hamling *et al.* 2009).

However, in anisotropic media, e.g. highly fractured/jointed/faulted rocks or rheological/compositional boundaries (see Fig. 1c, d), dykes follow paths of least resistance, i.e. least tensile strength, along pre-existing anisotropies (e.g. Gudmundsson 1984, 2011; Hou 2012). Such anisotropies are usually produced by earlier tectonics or by present-day far-field tectonic stresses and rarely by magmatic forces (Hou 2012 and references therein). Thus dyke emplacements also inherit pre-existing fabrics/anisotropies (Misra & Mukherjee 2015*b*); these dykes usually show specific signatures that indicate post-tectonic magma flow either through a fracture or coeval to fracturing (Fig. 1c).

Blyth (1949) identified dykes intruding fault/shear planes in South Galloway, Scotland. Relationships between dykes and pre-existing or active faults/brittle shears have also been well studied in other locations: e.g. near Washington (Cater 1982); the Middle Jurassic Concón Mafic Dyke swarm in Chile (Creixell *et al.* 2006); Paleogene dykes on Livingstone Island, Antarctica (Kraus *et al.* 2010); and Sierra de San Miguelito, Mexico (Xu *et al.* 2013). Watkeys (2002) identified dykes along pre-existing Y-, P-, R_1-, R_2- and T-planes (his fig. 11; Fig. 1e here for shear plane definitions), with dominant intrusions within Y-planes, in Karoo, South Africa. Such detailed studies have not been performed for the Deccan Traps, India.

Here, we describe detailed field relationships for 43 dykes and deformation structures from the western Deccan Large Igneous Province (DLIP) exposed around Mumbai (Maharashtra, India). Dyke–shear relationships from this region have been mentioned cursorily by Dessai & Bertrand (1995), Hooper *et al.* (2010) and Misra *et al.* (2014). Misra *et al.* (2014) analysed deformation primarily from brittle shears and faults in an extended area of the Western Deccan Strike-slip Zone (WDSZ). Misra *et al.* (2015) studied offshore structures and determined the sequence of ridge-jumps involved in the Seychelles–India separation. Here we concentrate on only the relationship between dykes and brittle shears and faults, which has not been studied in earlier work. This is important because we observed during our initial study that many dykes intrude brittle shears and faults. Thus, commenting the regional tectonic based on only dyke trends may be erroneous. To determine extension direction, only faults and brittle shear zones must be used for the WDSZ, principally because slip reorientation (see Philippon *et al.* 2015) should be at a minimum here as dip-slip, low-dipping normal faults are absent (see Misra *et al.* 2014 for details).

We use standard brittle shear nomenclature, e.g. P- and Y-planes (Fig. 1e–g) (Passchier & Trouw 2005, fig. 5.50; Mukherjee & Koyi 2010; Mukherjee 2013*a*, *b*, 2014*a*, 2015 for usage). Primary Riedel shear planes are designated as 'R_1', secondary Riedel shear planes as 'R_2' (Petit 1987) and tensile fractures as 'T' (e.g. Misra *et al.* 2015; Fossen 2016). P-, R_1-, R_2- and Y-planes form in brittle shear zones. T-planes can form perpendicular to the minimum horizontal compression direction (SH_{min}), even in sheared domains (Gudmundsson 2011). So the SH_{min} direction can directly be inferred from T-fractures, though such fractures are difficult to observe these in the Deccan Traps (e.g. Misra *et al.* 2014). Riedel shears are common in strike-slip domains but have also been reported from other shear zones (Davis *et al.* 2000; Katz *et al.* 2004).

Dykes and brittle deformation

Dyking can be pre-, syn- or post-tectonic. When dyking is pre-tectonic, subsequent structures are imprinted within the dykes, depending on their relative weakness compared to the rock matrix (Misra & Mukherjee 2015*b*). Unless earlier tectonic deformation has occurred, such intrusions are of type (i) mentioned earlier. On the other hand, when dyking post-dates tectonic deformation, type (ii) dykes may follow zones of least resistance and intrude pre-existing tectonic deformation planes: here, Y and P. However, if the host rock is weaker than the heterogeneities, or if the tectonomagmatic stress is not strong enough to intrude into the anisotropies, type (i) dyking may occur (e.g. Hou 2012; Martínez-Poza *et al.* 2014).

In the Vestfold Hills, Antarctica, Hoek (1991) identified a 'zig-zag' pattern of dykes in response to host rock containing one or two sets of pre-existing planar anisotropic elements. Dilation in such cases is normal to the dyke envelope (Fig. 1d). In contrast, dilation for en echelon dykes is oblique to the dyke envelope (Hoek 1991).

Ziv *et al.* (2000) examined recent dyke intrusions in basaltic host rock through pre-existing fractures in Kilauea, Hawaii and established that at least one of the following criteria must be satisfied to direct a dyke through a fault: (a) the σ_3 (extension) direction related to dyke intrusion is at a high angle to the fracture; (b) the resolved shear stress in any direction along the fracture during intrusion is less than the magma overpressure, to allow its flow – in other words, the ratio of brittle to ductile shearing along the dyke margins is less than the dilation of the country rock due to dyking; and (c) the tensile strength of the host rock exceeds the effective ambient dyke-normal stress.

Many mafic dykes within host rocks comprising basalts, agglomerates, tuffs, etc. in Iceland intrude pre-existing faults and fractures (e.g. Opheim & Gudmundsson 1989; Gudmundsson 2011). Dykes are boundaries between weak (e.g. pyroclastic rocks) and strong (e.g. basaltic layers) lithologies (Gudmundsson 2003; Gudmundsson & Loetveit 2005). Many dykes originating from deep crustal magma chambers remain blind and are not feeder dykes (Gudmundsson 2006; review in Gudmundsson 2011).

Cadman *et al.* (1993) showed that many dykes in the Labrador region (Eastern Canada) intruded during either tensile fracturing or brittle shear. A family of dykes acted as incompetent layers during further deformation, and shears later localized within those dykes. Pyroclastic dykes of central Mexico (Torres-Hernández *et al.* 2006) and basaltic dykes in South Nevada, USA (Valentine & Krogh 2006) were emplaced at shallow depth along pre-existing regional normal faults. Pyroclastic dykes of central Mexico were also emplaced along pre-existing Riedel shears (Xu *et al.* 2013). In the dyke swarm within the Karakoram shear zone, Ladakh (India), dykes follow various pre-existing anisotropies, e.g. brittle shear planes, foliation planes or fractures (Reichardt & Weinberg 2012).

Steeply dipping faults and fractures efficiently guide dykes upwards (Gaffney *et al.* 2007). Kavanagh & Sparks (2011, figs 4 & 5) demonstrated that most of the dykes in the kimberlite Star dyke swarm (South Africa) intrude steeply dipping pre-existing fractures within the dolerite host rock. Volcanic intrusions and vents run parallel to rift-related structures in the Tanzania divergence area, East African Rift System (Isola *et al.* 2014, fig. 4). The vent density is higher along the Y- and R-shear planes (Isola *et al.* 2014, fig. 5). Trippanera *et al.* (2015) demonstrated that dykes in recent, active magmatic divergent plate boundaries in Iceland and the East African Rift System terminate in fissures and faults at shallower levels. These dykes may be used to explain graben formation and long-term rift evolution.

Creixell *et al.* (2006) demonstrated – using field radiometric, petrographic and anisotropy of magnetic susceptibility (AMS) data – that the Jurassic Concón Mafic Dyke Swarm, in central Chile, was emplaced during sinistral shear of the Paleozoic host rock granitoids. Such results were also obtained for shearing coeval dykes by Féménias *et al.* (2004) in Romania and Clemente *et al.* (2007) in the Canary Islands, Spain.

Syn-kinematic dykes may vary laterally in mineralogy, geochemistry and strain (Zulauf & Helferich 1997). Syn-deformation dyking usually produces typical fabric, as reported from East Brazil (Correa-Gomes *et al.* 2001). Correa-Gomes *et al.* (2001) recognized two types of fabric related to dykes: (a) symmetric fabric, when dyking occurs along a pre-existing fault; and (b) asymmetric fabric, for dyking within an active fault. The degree of

Table 1. *Stratigraphy of the Deccan Large Igneous Province*

Sub-group	Formation		Dominant lithology
	Lithostratigraphy	Chemostratigraphy	
Salsette	Borivali	Mumbai volcanics	Trachytes, rhyolites, tuffs, agglomerates, and intertrappeans, etc.
Wai		Desur	Fine- to medium-grained, moderate to sparsely porphyritic flows
	Mahabaleshwar	Panhala	
		Mahabaleshwar	
	Purandargarh	Ambenali	
	Diveghat	Poladpur	
	Elephanta		
Lonavala	Karla	Bushe	Fine- to medium-grained aphyric flows
	Indrayani	Khandala	
Kalsubai	Ratangarh	Bhimashankar	Dense aphyric to phyric flows with moderately porphyritic pahoehoe flows
	Salher	Thakurwadi	
		Neral	
		Igatpuri	
		Jawhar	

After Beane *et al.* (1986), Mitchell & Widdowson (1991), Godbole *et al.* (1996), Widdowson *et al.* (2000), Vaidhyanadhan & Ramakrishnan (2008), Renne *et al.* (2015); lithologies from District Resource Maps of Mumbai, Thane, Raigad, Ratnagiri, Pune districts, and Geological Survey of India 2001; see Figure 2 for occurrence of the Formations.

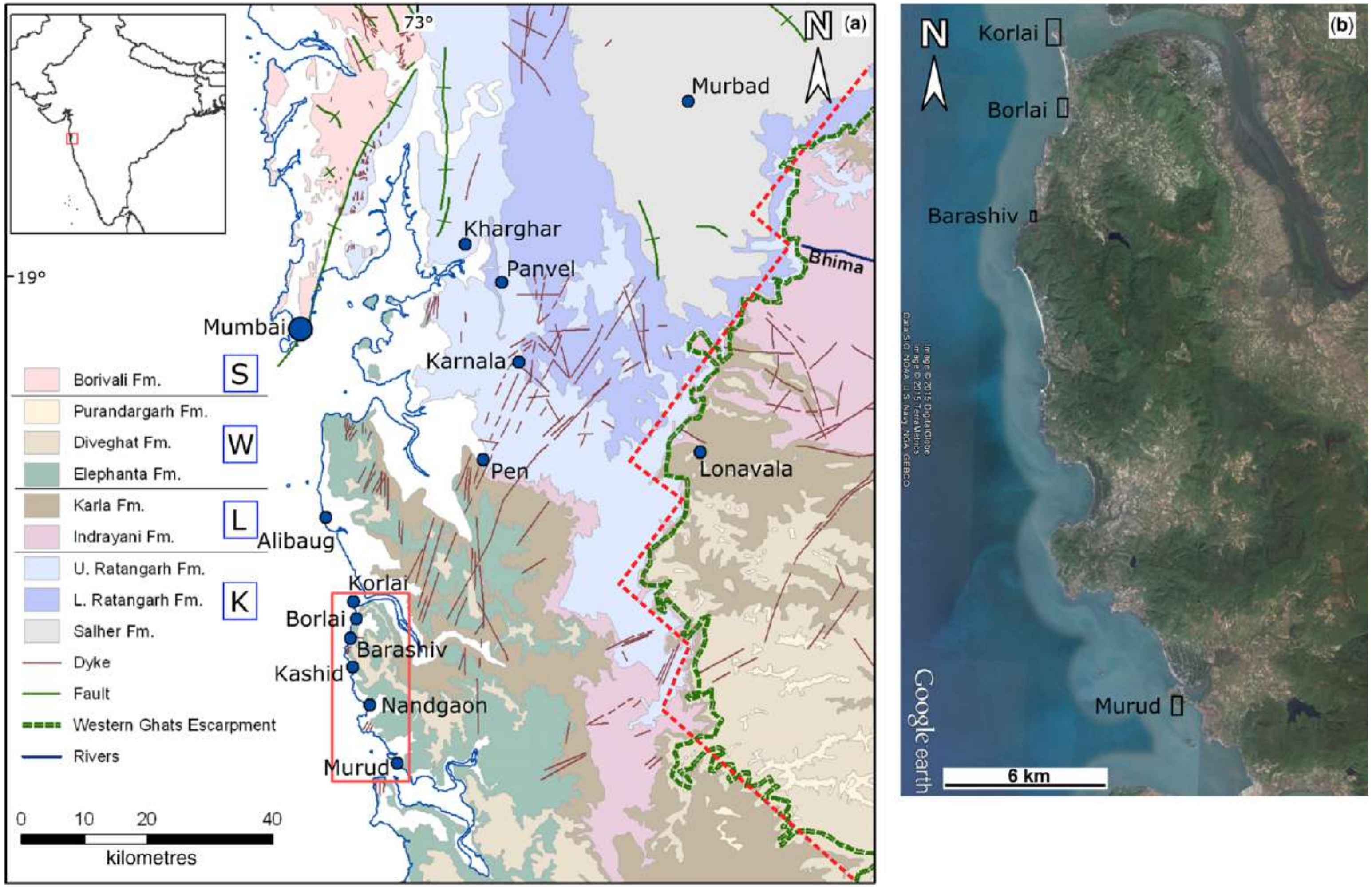
(a)
73°
19°
N
Murbad
Kharghar
Panvel
Mumbai
Karnala
Bhima
Pen
Lonavala
Alibaug
Korlai
Borlai
Barashiv
Kashid
Nandgaon
Murud
S
W
L
K
Borivali Fm.
Purandargarh Fm.
Diveghat Fm.
Elephanta Fm.
Karla Fm.
Indrayani Fm.
U. Ratangarh Fm.
L. Ratangarh Fm.
Salher Fm.
Dyke
Fault
Western Ghats Escarpment
Rivers
0 10 20 40
kilometres
(b)
N
Korlai
Borlai
Barashiv
Murud
6 km
Google earth

symmetry is conventionally analysed by the angular relation between the dyke symmetry plane (an imaginary plane longitudinally separating the dyke into two equal parts) and the fabric symmetry plane (bisecting the trends of the fabric elements near the margins). Correa-Gomes *et al.* (2001) also presented field criteria (Fig. 1c) in order to identify fabrics formed during syn- to post-deformational intrusion. They included grooves, branching, drag folds, Riedel fractures, P-shears and plumose marks at the dyke margins.

Regional geology

Deccan Large Igneous Province

The DLIP, or the Deccan Traps, is one of the largest large igneous provinces (LIPs) on Earth. It originated when the Indian plate drifted over the Réunion hotspot during the Late Cretaceous to Paleocene. The cumulative age of the DLIP-related rocks within the Indian mainland is *c.* 68–60 Ma (Chenet *et al.* 2007 and references therein). Deccan lava flowed over a long period of time, and not as a single short pulse (review by Chandrasekharam 2003). DLIP rocks cover >500 000 km^2 of peninsular India. The Indian rift basins of Barmer (Rajasthan), Cambay and Kachchh (Gujrat), Narmada (Madhya Pradesh, Maharashtra and Gujrat) and Mumbai (Maharashtra) also have buried/exposed DLIP-related rocks. The DLIP consists of grey to blackish, medium- to fine-grained basalts and dolerites (e.g. Deshpande 1998). In addition, there are also alkali basalts, high Mg-basalts (such as basanite and picrite), nephelinites, carbonatites, rhyolites, lamprophyres, andesite, granophyre and obsidian, etc. (reviews by Vaidhyanadhan & Ramakrishnan 2008; Valdiya 2016). The individual flows are usually horizontal and tabular, and are remarkably laterally continuous, at >100 km (Deshpande 1998). The total flow thickness exceeds 2000 m near the Indian west coast. Thickness decreases towards the east and south, producing flat-topped hills with characteristic stair steps. Table 1 presents the lithostratigraphy and chronostratigraphy of the western DLIP. These rock units occur in the WDSZ (Fig. 2a).

Seychelles separated from India at *c.* 63–62 Ma (Collier *et al.* 2008; Bhattacharya & Yatheesh 2015; Misra *et al.* 2015). The Seychelles–India oblique separation formed the WDSZ, which has been traced for *c.* 150 km from Jawahar to the north to Harihareshwar to the south, based on fieldwork supplemented by remote sensing (Misra *et al.* 2014). This brittle shear zone, which is devoid of gouge and breccia, extends from the Western Ghat Escarpment in the east up to the west coast. The north and south extents of the WDSZ await delineation. The zone is characterized by slickensides bearing subvertical, approximately NE–NW-trending and N–S-trending fault planes, extension joints, pull-apart structures, etc. (Dessai & Bertrand 1995; Hooper *et al.* 2010; Misra *et al.* 2014; Misra 2015). Approximately N–S-trending extensive palaeostress has been deduced from faults and brittle shears in the WDSZ. Supplementary Figure S1 shows palaeostress inversions from faults and brittle shears in the study area. Around the WDSZ the Deccan Traps were emplaced over the Western Dharwar Craton; this has been shown by xenolith studies and wells drilled around the Koyna region, *c.* 150 km southeast of the study area (Ray *et al.* 2008; Rao *et al.* 2013; Roy *et al.* 2013; Upadhyay *et al.* 2015).

Dykes in the Deccan Large Igneous Province

Dykes occur throughout the DLIP. However, they are denser to the west and north and almost absent from the central area (Deshmukh & Sehgal 1988). Whether the Deccan dykes are feeders to lava flows has been debated (Chandrasekharam 2003), and they may have facilitated the supply of lava in the final phases of Deccan volcanism (Hooper *et al.* 2010; Vanderkluysen *et al.* 2011). However, direct field evidence for a feeder–flow relationship is scarce (Auden 1949; Deshmukh & Sehgal 1988) and instead there may have been post-volcanic hypabyssal injections such as sills and other intrusives fed by dykes (e.g. Agashe & Gupte 1972). Dykes in India's west coastal region of the Deccan Traps and Nashik–Pune correlate geochemically with the younger Poladpur, Ambenali and Mahabaleshwar Formations and possibly acted as feeders to those flows (Vanderkluysen *et al.* 2011).

Three dyke swarms have been identified in the DLIP: (i) the ENE–WSW-trending Narmada–Tapti swarm; (ii) the N–S-trending West Coast swarm, occurring mainly in the WDSZ; and (iii) the weakly oriented NNE–SSW to NE–SW

Fig. 2. (**a**) Map of the study area with field locations (modified from Misra *et al.* 2014). The Formation (Fm.) in part of the WDSZ are shown. Key locations are shown as blue dots. The main study area is shown in the red rectangle. Other field areas where data could be collected are Kharghar and Karnala. Sub-groups are stated in blue squares alongside the Formations: K, Kalsubai; L, Lonavala; W, Wai; S, Salsette. Red dotted line: possible eastern boundary of the WDSZ. (**b**) Google Earth image of the area marked with a red rectangle in (a), with the main field locations marked with black rectangles. The areas in the black rectangles are further shown in Figure 3.

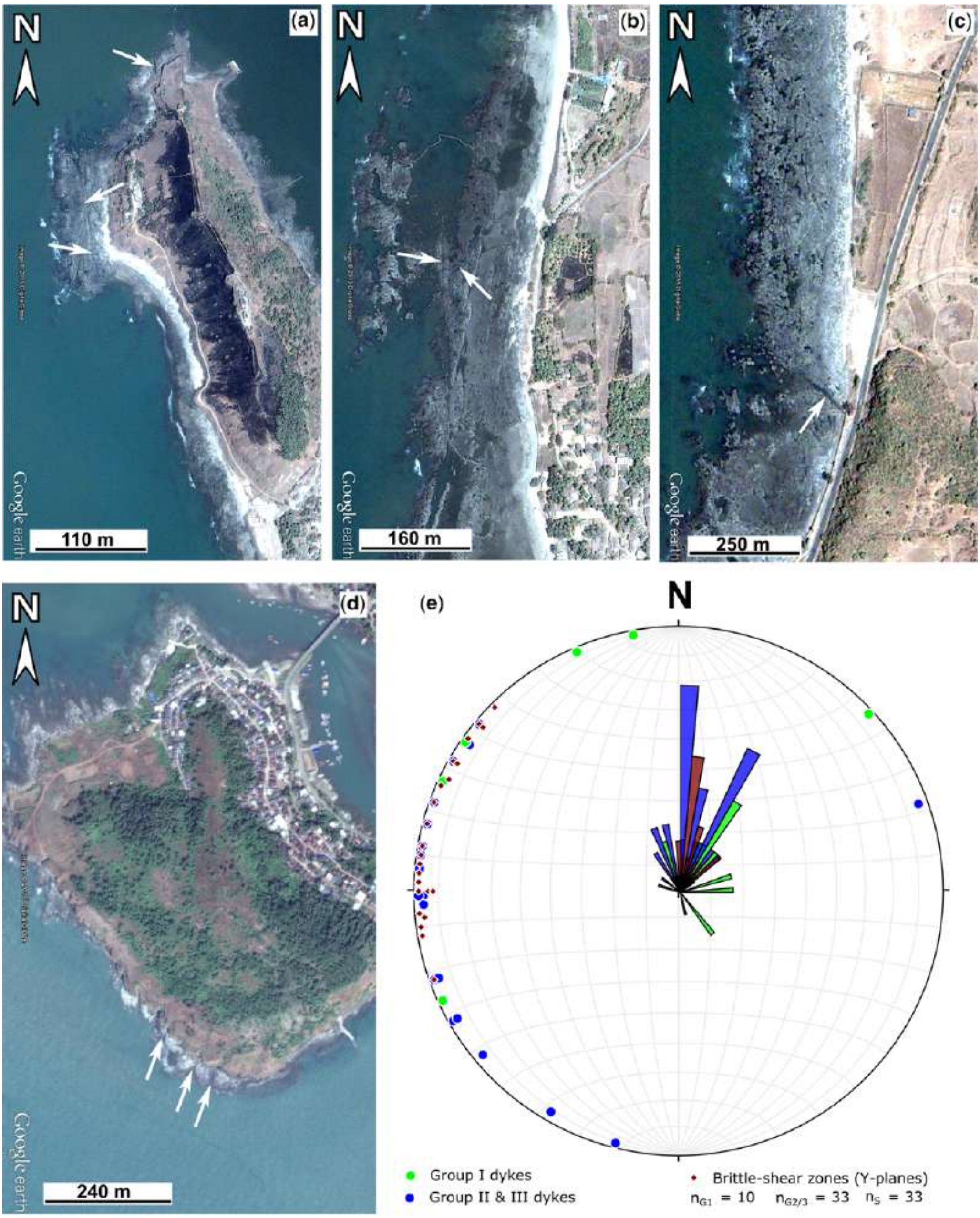

Fig. 3. Google Earth images of the main field areas: (**a**) Korlai, (**b**) Borlai, (**c**) Barashiv, and (**d**) Murud. White arrows: dykes visible on satellite images. Dyke in (c) is dyke 2 in Figure 9c. Dykes are identified by darker linear markers in some cases, as in (c). In many places dykes are eroded and only linear depression implies the presence of a dyke. Therefore, dykes are also identified by linear gullies, such as in Korlai (a) (upper arrow) and Murud (c) (all arrows). (**e**) Pole plot and frequency–azimuth rose diagram of dykes in the study areas as shown in Figure 3a–d. Group I dykes are faulted or sheared (pre-deformation intrusions); group II and III dykes intrude into shear zones or bear P-, R- and Y-planes along their margins (post- or syn-deformation intrusions). n_{G1}: number of dykes in group I; $n_{G2/3}$: number of dykes in groups II and III; n_S: number of shear zones/faults. Note the strong match of the group II and III dykes and brittle shears. Also note the lack of strong orientation in the group I dykes.

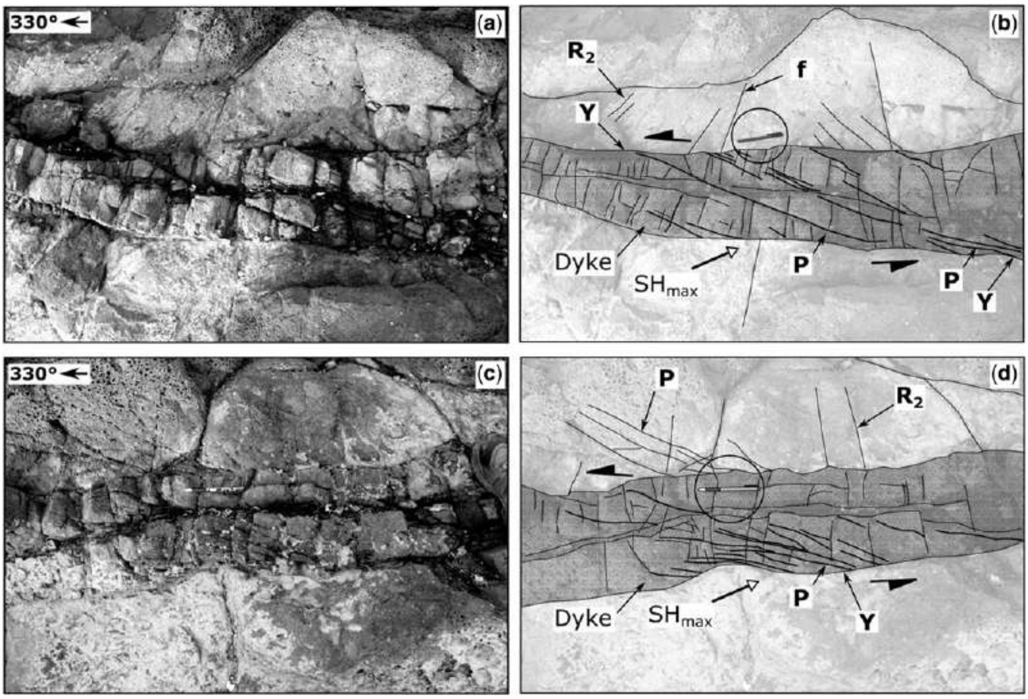

Fig. 4. Shears along the boundaries of dykes at sub-horizontal outcrops at Korlai (Figs 2 & 3 show locations). (**a**) Uninterpreted; (**b**) interpreted: P-shears (bold lines) are present through most of the width of the *c.* 30 cm thick dyke. However, the shears do not reach the other margin. The dyke is divided longitudinally by a conspicuous fracture, which also cross-cuts one of the P-shears. Other fractures are marked by thin lines. (**c**) Uninterpreted; (**d**) interpreted: P-shears (bold lines) are present along both dyke margins and do not cross-cut the longitudinal fracture. There are some P-shears in the host rock indicating dragging along the dyke margin during intrusion. There are fewer possible R_2 Riedel shears than P-shears. They appear simply as brittle planes, and no associated sigmoid brittle plane is seen. Note fracture 'f': not all fractures can be interpreted using well-known terms such as Y- and P-, etc., and other types are avoided in discussion. This is standard practice in structural geology. The 13 cm pens are markers (circled).

Nasik–Pune dyke swarm (Deshmukh & Sehgal 1988; Bondre *et al.* 2006; Ray *et al.* 2007; review by Valdiya 2011). Average extension calculated from the dykes is approximately 30% (Dessai & Bertrand 1995), 18% (Bhattacharji *et al.* 1996) and 4–5% for a selection of small areas (Ju *et al.* 2013; review in Valdiya 2016). Misra (2008) stated that the ENE–WSW dyke swarm is abruptly truncated by N–S faults.

We studied the West Coast dyke swarm around Mumbai and nearby regions (Figs 2 & 3). The dominant dyke trend is approximately N–S, although some trend NW–SE to NE–SW and rarely E–W (Misra *et al.* 2014; Misra 2015). Dessai & Bertrand (1995), Hooper *et al.* (2010) and Misra *et al.* (2014) report on the dykes and their relationship with the deformation structures in this area. Three sets of dykes have been identified geochemically and geochronologically (Dessai & Viegas 2010; Hooper *et al.* 2010). The dominant trends for two of these sets are approximately N–S and are parallel with and either intrude or obliquely cut the Y-planes (Hooper *et al.* 2010; also field photographs by Dessai & Bertrand 1995; Misra *et al.* 2014). The third set has a weak WSW–ENE to N–S trend and predates the shear zones (Fig. 3e; Hooper *et al.* 2010). The dyke sets have been dated at 66–65, *c.* 65 and 65–63 Ma (Hooper *et al.* 2010 and references therein). Based on major and trace element isotopic ratios, the dykes are weakly related to the Bushe, Poladpur, Ambenali and Mahabaleshwar Formations, and many do not link with any DLIP Formation. It is possible that some of these flows have been eroded (details in Vanderkluysen *et al.* 2011).

Dykes and brittle shear

We studied Deccan dykes and brittle shear at the rocky beaches/wave-cut platforms at Korlai, Borlai,

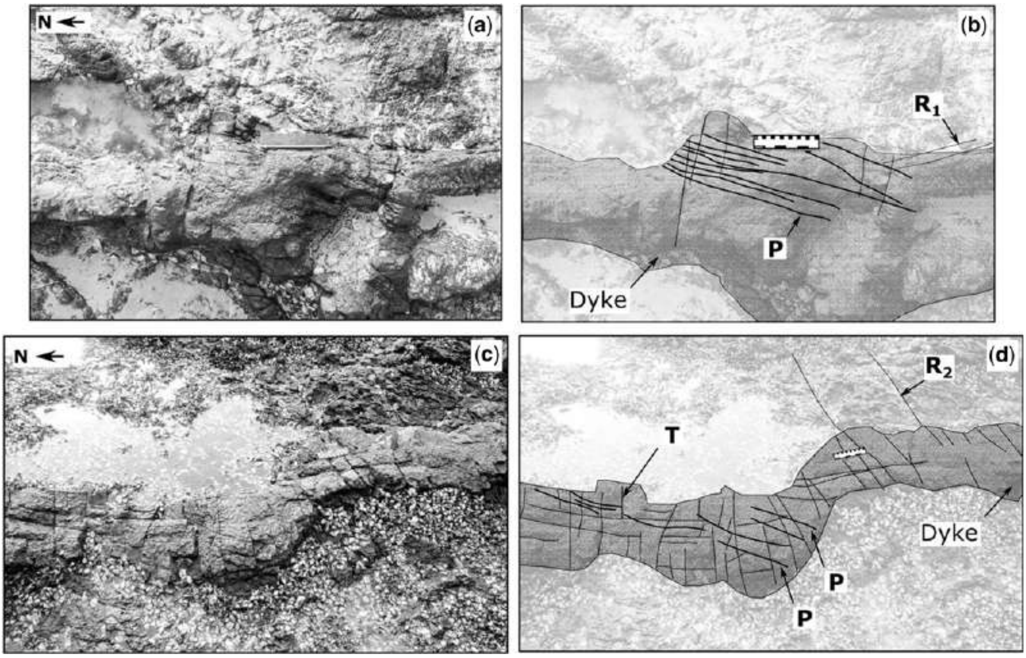

Fig. 5. Shears along the curved/irregular boundaries of dykes at sub-horizontal outcrops at Borlai (Figs 2 & 3 show locations). (**a**) Uninterpreted; (**b**) interpreted: P-shears (bold lines) confined near the dyke margin(s). This dyke is devoid of tensile (T) fractures. (**c**) Uninterpreted; (**d**) interpreted: P-shears (bold lines) along a dyke margin. This dyke is curved because of a possible top-to-left and down shear sense. This dyke had numerous tensile (T) fractures with P-shears. This dyke is curved, indicating intrusion along a pre-existing approximately NW-trending fracture. At the left of the figure the T-joints are nearly perpendicular to the longitudinal joints. However, at the right the T-joints are not orthogonal to the shear, and a sinistral shear sense is indicated that matches the inclination of the P-planes. The right part of the figure shows a block/lens of rock produced with almost sigmoid shape. This behaviour of variation in T-planes along the length of the dyke indicates possible strain partitioning. The Y-planes are not clearly visible in these examples, and bulk shear sense is not indicated in such areas. Possible R_1 and R_2 Riedel shears are also present, but there are fewer of these than P-shears. They appear only as brittle planes and no associated sigmoid brittle plane was seen. The 15 cm long scales are markers. Both photographs are courtesy of Abhimanyu Maitra.

Barashiv and Murud (Figs 2 & 3), south of Mumbai city (Fig. 2 for locations). Most of the observations were made at near-horizontal sections. Dykes belonging to the coastal swarm, in Kharghar and Panvel, were also mostly studied at subvertical exposures. Upadhyay *et al.* (2015) observed xenoliths in a coastal swarm dyke north of the study area, but within the WDSZ. However, we did not observe xenoliths in the dykes that we studied. Thus it is probable that either thermal erosion (Groves *et al.* 1986; Fialko & Rubin 1999; Valentine & Krogh 2006) along the dyke margins was minimal or small xenoliths were completely assimilated. Geshi *et al.* (2010) identified feeder dykes where the dykes finally became flow layers. Dykes that abruptly terminate at a mechanical boundary, e.g. a scoria layer or flow boundary, can be non-feeders. We observed only two such non-feeder dykes in a subvertical section, one each at Korlai and Murud (Fig. 2 for locations), and those were *c.* 15 cm thick. The P-planes were at 20–40° to the Y-planes. The primary Riedel shears (R_1) were at 10–30° to the Y-planes and cross-cut them. The T-planes were at *c.* 30° to the Y-planes and were truncated by them.

Here we discuss deformation structures observed at outcrops that establish the relationship between dykes (of the coastal swarm) and brittle shears.

(1) Shears at the dyke margins: approximately N–S-trending P-shears and, rarely, N–NE-trending primary Riedel shears (R_1) were seen along the margins of some dykes (Figs 4–6). This is similar to fig. 5 in Blyth (1949). P-shears end tangentially at the dyke margin, and R-shears continue from the dyke into the host rock. The dyke margins act as Y-planes, with dominant approximately N–S trends, with some trending NE–NW.

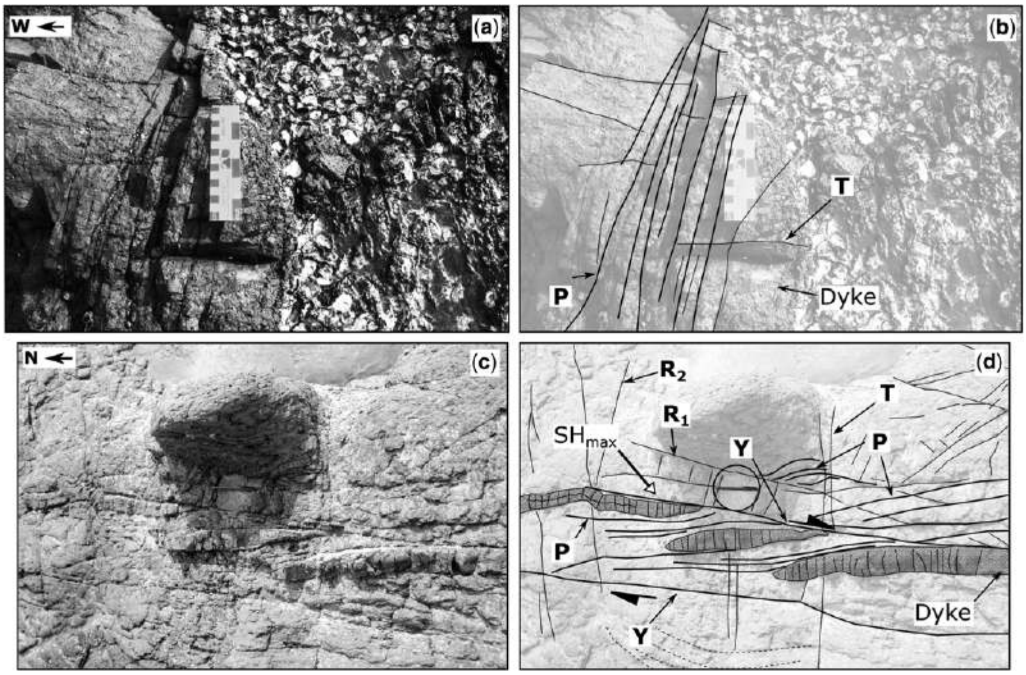

Fig. 6. Examples of brittle shear–dyke relationships at sub-horizontal outcrops. (**a**, **b**) Borlai (Figs 2 & 3 for locations): P-shears (bold lines) along the margin of a dyke with tensile (T) fractures. The 15 cm scale is a marker. Photograph is courtesy of Abhimanyu Maitra. (**c**, **d**) Korlai (Figs 2 & 3 for locations): the *c.* 3 cm thick dyke intrudes P-planes and one Y-plane. The intruded shear planes were possibly the weakest amongst all those present (Fig. 1a). This represents a clear instance of post-deformation intrusion. Possible R_1 and R_2 Riedel shears are present, but there are fewer of these than P-shears. They appear only as brittle planes, and no associated sigmoid brittle plane is seen. At the bottom of (c), sub-rounded fractures can be seen (dotted lines). Those are possibly related to spheroidal weathering, and are atectonic; they are not used in this study. In the upper part a subrounded spheroidally weathered core can also be seen. The 13 cm pens are markers (circled).

Fractures, equidistant from and parallel to each other, are observed; these are (a) confined within the dykes (cooling related); (b) in the host rock (tectonic, i.e. T-fractures); and (c) continuous in the host rock and dykes (T-fractures). T-fractures in the country rock are also perpendicular to the dyke margins. They are subvertical and approximately E–W trending (Fig. 4b). T-fractures are seldom weakly sigmoid, possibly indicating post-intrusion shearing along the dyke margins. In some cases there is fracturing parallel to the dyke margins, which divides the dyke longitudinally into two sub-equal parts. Such longitudinal fractures have been observed in dykes elsewhere, e.g. the Ethiopian LIP (Mège & Korme 2004). They indicate gradual inward cooling. Where shear Y-planes are observed, they indicate shearing along the dyke (e.g. Mège & Korme 2004). Longitudinal and transverse fractures are reported from the DLIP and are usually associated with cooling (Ray *et al.* 2007, fig. 2; Sheth *et al.* 2014, fig. 3). Cross-joints/fractures are nearly straight and almost perpendicular to the dyke margin (Jerram & Petford 2012, fig. 6.6). Shears are seldom present on both sides of the longitudinal fractures (Fig. 4c, d). Shears at the edges of the dykes are reliable examples of syn-tectonic intrusion (e.g. Correa-Gomes *et al.* 2001; Creixell *et al.* 2006). Some *c.* 30 cm thick dykes display curved P-planes restricted within the dykes and near their margins (Fig. 5a, b) and also through most of the dyke body (Fig. 5c, d). Dominantly E-trending and occasionally approximately NE–NW-trending tensile fractures often accompany the P-planes (Figs 5c, d & 6a, b). Sengupta (1997) also reported shear zones at the dyke–country rock interface at Schirmacher Hills, Antarctica. This resembles 'wall-rock drag' (Fig. 1d). Sometimes the possible P-shears are at a low angle (10–20°) to the dyke margin or Y-shears (e.g. Fig. 6a, b).

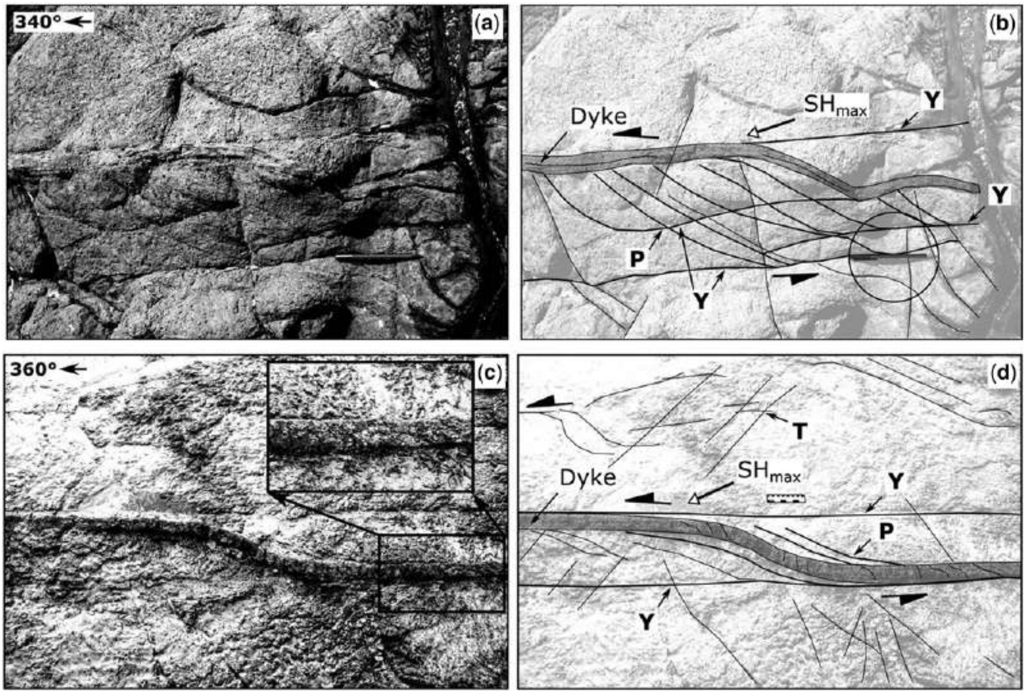

Fig. 7. Examples of dykes intruding brittle shears at sub-horizontal outcrops. (**a**, **b**) Korlai: a near-symmetric rhomboid rock slice bounded by P- and Y-shear planes does not give accurate shear sense, so is not used in interpretation. Longitudinal joints concordant to the curved dyke are present. The 13 cm pen is a marker (circled). (**c**, **d**) Borlai (Figs 2 & 3 show locations): P- and Y-shears (bold lines) in the host rock basalts. The dyke intrudes Y-shears, diverts through P-planes and then intrudes the Y-shears again. These are possibly some of the best examples of post-deformation intrusion. The inset in (c) is zoomed in to show sigmoid cross-joints. It is assumed that these were previously straight (Fig. 4a–d), but attained a sigmoid shape due to shearing. The same shear sense (or synthetic) as bulk shear is indicated. The 15 cm scale is shown as a marker. Photographs in (c) and (d) are courtesy of Abhimanyu Maitra.

Such shears are not used to determine shear sense. In places, the dykes are sigmoid shaped, like ‘mineral fish’, in ductile shear zones (Fig. 6c, d), as described by Mukherjee (2011).

(2) Dykes within P- and Y-planes: while point (1) above deals with shears within or at the dyke margins, here we present centimetre-scale dykes intruded within the Y- or P-planes (Figs 6c, d & 7) or parallel to the Y-planes (see Fig. 1e for shear criteria and nomenclature). As shown in Figure 6c and d, an en echelon dyke geometry may appear due to tectonic deformation, as in the case of gash veins. However, in this case, the straight or planar segments of the dyke do not match the en echelon pattern. Moreover, there are very well-developed Y-planes that envelope the P-planes. Angles between the Y- and P-planes are in the range 20–30°. All these fractures would have been of the ‘opening’ type (mode I), with intrusion or mineralization within them. We see only two segments that are en echelon and intruded (Fig. 6c, d). This is rather a brittle shear zone, where intrusion took place along the Y- and P-planes (brittle shear nomenclature in Fig. 1e). Not all fractures are filled by melt, because there is usually a compressive field surrounding the dyke during intrusion. The shears trend approximately NNW–N. The approximately E-trending T-fractures in the host rock are subvertical. Thinner dykes are presumably more sensitive to changes in the P- and Y-plane trends and intrude along them (Fig. 7a–d). In some cases the thin dykes are parallel to the approximately NE-trending Y-planes, and in other cases they reside between the P- and Y-planes (Misra *et al.* 2014, fig. 15). In these cases, the dykes occupy neither the Y- nor the P-plane but appear between the two planes and are parallel to the Y-plane.

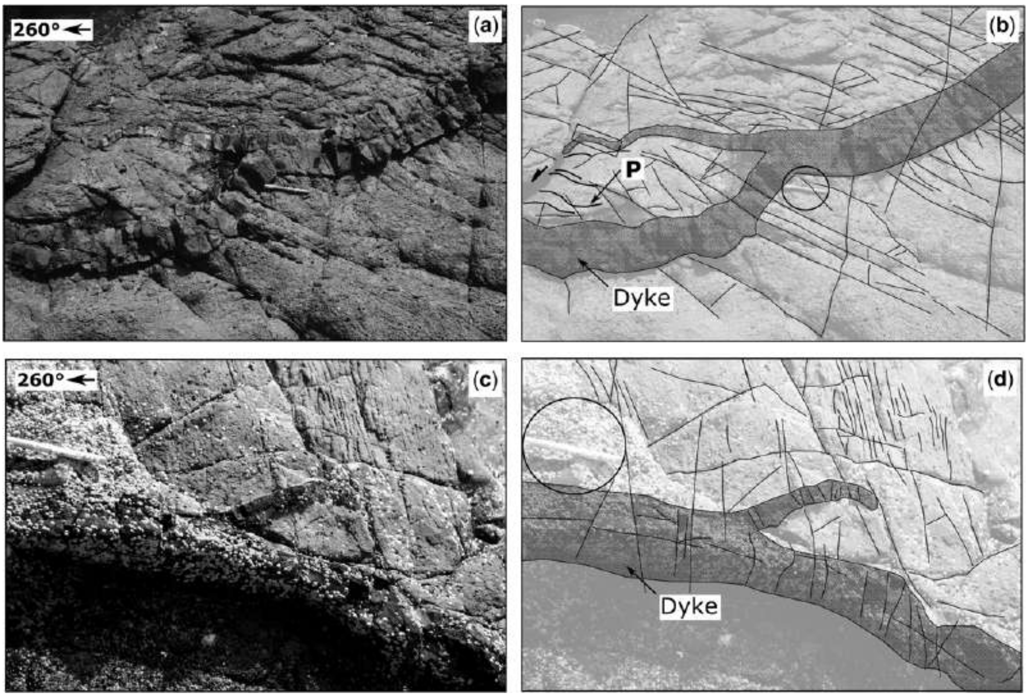

Fig. 8. Examples of branches/horns/apophyses in dykes at sub-horizontal outcrops at Korlai (Figs 2 & 3 for locations). (**a**, **b**) A branch possibly intrudes pre-existing fractures. Sigmoid P-planes (marked by an arrow) near the branch have the same sinistral shear sense (single half arrow) as the branch itself. That means that the dyke may have occupied one of the sigmoid P-planes. (**c**, **d**) The branch does not intrude any fracture in its vicinity. Branches may indicate syn- or post-deformation intrusion. However, they are not the best examples for such an interpretation. The 13 cm pens act as markers (circled).

Sheth & Cañón-Tapia (2015, figs 2b & 5b) also showed that approximately N–S-trending dykes possibly intruded into Y-planes at Borlai Korlai (location shown in Fig. 2), although they did not recognize those planes as 'Y'. Dykes may occupy the Y-plane through some length (Misra *et al.* 2014, fig. 15a). This also indicates possible post-tectonic intrusion. Dykes thicker than 1 m exhibit such a relationship in this region. Misra *et al.* (2014, fig. 14c) document >50 m thick dykes intruding both the 40° striking Y-plane and its corresponding 30° striking P-plane, approximately 4 km north-west of Murbad (location in Fig. 2), as observed in satellite images. These observations may be considered good evidence of post-tectonic dyking.

(3) En echelon dykes in a shear zone: dykes with thickness of <5 cm appear in an en echelon pattern within P- and Y-planes in shear zones at Korlai and Borlai (Fig. 6c, d). Some of the individual segments of the dykes occupy the P-planes close to each other, and other segments occupy the Y-planes or are parallel to them. This is a good example of post-tectonic intrusion. The general trend of the Y-planes is approximately N, and the P-planes trend approximately NW. The brittle shear zone in Figure 6d has a dextral shear sense, which is different from the sinistral shears commonly observed in this region (Misra *et al.* 2014). It is usual to find a few reverse shears in shear zones worldwide. Local approximately NE–SW extension is indicated from this brittle shear zone. The centimetre-scale offset in the dyke segments is caused by the dyke following P-planes. The distance between the P- and Y-planes varies widely, from a few centimetres (Figs 6c, d & 7a–d) to a few metres in places, although only one instance of this degree of separation can be seen. The 2–5 cm thick dykes are also cross-jointed, and one set of these joints, perpendicular to the dyke margin, does not continue into the host rock. It is possible that these are cooling joints (see Budkewitsch & Robin 1994; Gudmundsson 2011).

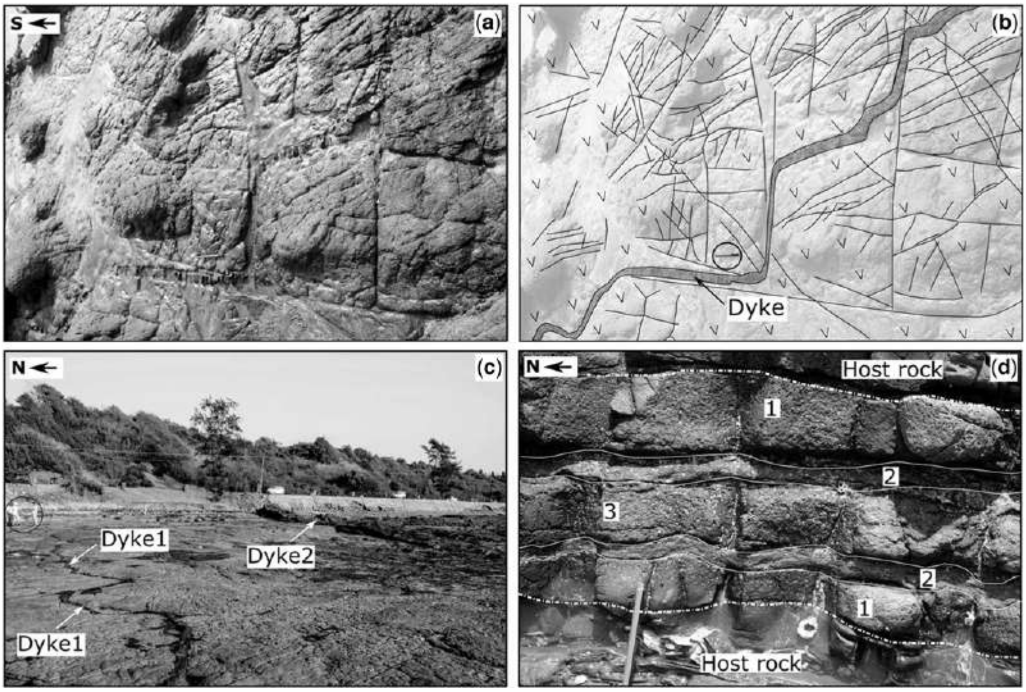

Fig. 9. (**a**, **b**) A *c.* 3 cm thick approximately N–S trending dyke intrudes numerous fractures within the host rock at a sub-horizontal outcrop at Korlai (Figs 2 & 3 show locations). Mutually perpendicular fractures are mostly intruded. A 13 cm pen acts as a marker (circled). (**c**) The Barashiv sub-horizontal outcrop (Figs 2 & 3 show locations). Dyke 1 is *c.* 15 cm thick, trends approximately NW, and follows many pre-existing fractures. (a–c) are similar to Figure 1d. This dyke is also faulted in places, indicating continuing deformation after intrusion (see Fig. 10a, b for faults in the same dyke). Two geologists act as markers (circled). Dyke 2 is 2–3 m thick, trends approximately NW and has withstood erosion. This dyke can be seen on the satellite image in Figure 3c. (**d**) Multiple sub-parallel dyke intrusions at a sub-horizontal outcrop at Korlai (Figs 2 & 3 show locations), with prominent cross-fractures that have greater aperture than those in Figure 4a–d. 1, First intrusion phase; 2, baked zone of second intrusion phase; 3, second intrusion phase. This indicates at least two phases of intrusion with considerable temporal gap. Visible length of pen: 10 cm.

(4) Apophyses/horns: these are short dyke branches located at the tips and sometimes edges of dykes of any thickness (Hoek 1991; Correa-Gomes *et al.* 2001; Martínez-Poza *et al.* 2014). Horns form either by stress perturbations at the dyke tip or by melt migration through pre-existing fractures with diffuse terminations. Apophyses in the study area appear to intrude pre-existing fractures (Fig. 8a, b); secondary joints within the host rock continue within the dyke (Daniels *et al.* 2012, fig. 2b), but the apophyses intrude them. This forms complex dyke–fracture interaction, and the relative time between fracturing and intrusion is as yet unknown. Apophyses can also be unrelated to nearby brittle features (Fig. 8c, d), indicating that deformation post-dated intrusion. In some cases fractures in the country rock are parallel to dykes, and in these cases digitations are intensely structure controlled (Fig. 8a). However, this is not always the case where the country rock has a low density of fractures near the dykes (Fig. 8c). The P-planes in Figure 8a and d are not enveloped/bound by the Y-planes.

(5) Dykes intruding pre-existing anisotropies, excluding faults/brittle shears: thin (<15 cm) dykes enter all weak anisotropies in the host rock (Fig. 9), and still thinner dykes (<5 cm) enter contrasting N–S and E–W fractures without much change in thickness (Fig. 9a, b). There are pre-existing tensile fractures, cooling joints and brittle shears, etc., but dykes intrude only those anisotropies orthogonal to them. Slightly thicker (*c.* 15 cm) dyke geometries are even more irregular in locations such as Barashiv (Fig. 9c; location in Fig. 2), and these dykes follow almost

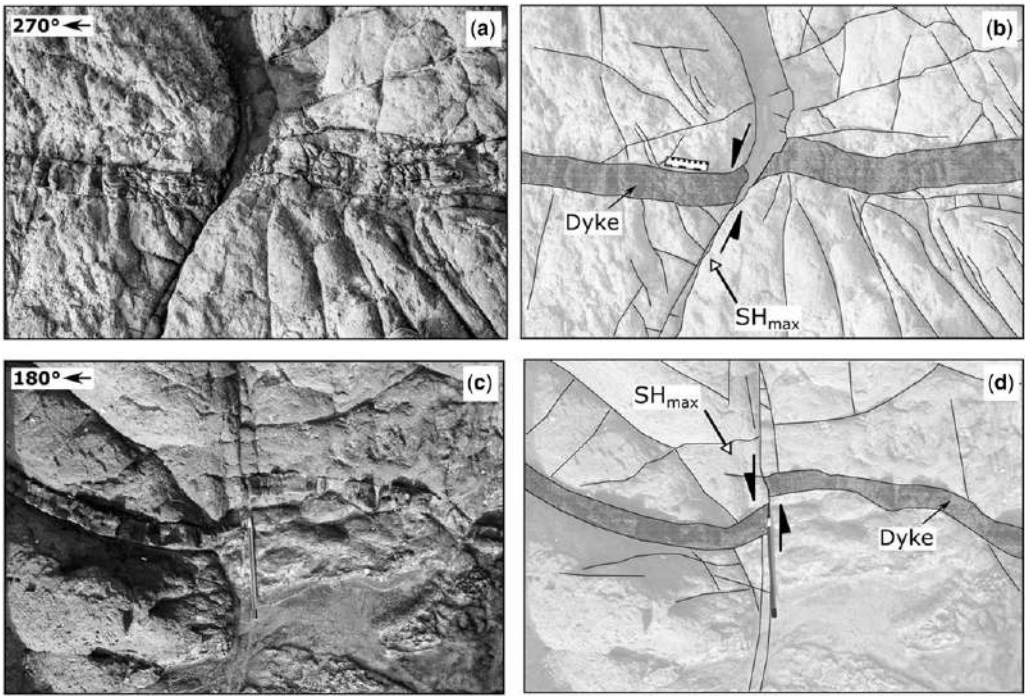

Fig. 10. Faulted dykes at sub-horizontal outcrops. (**a**, **b**) At Barashiv and (**c**, **d**) at Korlai (Figs 2 & 3 show locations). In both cases: (i) the intensities of drags of dykes across the faults are different; and (ii) normal dragging pattern (Passchier 2001; Mukherjee & Koyi 2009). The shear sense is determined from the relative slip of the dykes as markers. Other fractures are random and cannot be classified into shear sense indicators, so they were not used to determine the shear sense here. The 15 cm scale acts as a marker in (a) and (b) and the 15 cm pencil acts as a marker in (c) and (d).

all types of fracture. Thin dykes thicken or become even thinner, to 2–15 cm, maintaining an average approximately NW trend. However, these are not pinch-and-swell structures and do not indicate any tectonic pure shear perpendicular to their lengths. First, if they were pinch-and-swell structures, rock foliation would have produced drag folds at the pinches. However, the host rock (basalt) is non-foliated. Second, if they were pinch-and-swell structures, the possible compression/extension direction would not match the regional tectonics (Misra *et al.* 2014). Third, even if the rock were non-foliated, pinching and swelling would produce a new fabric that would show sucking towards the pinches (unpublished observations, S. Mukherjee), but no such features were observed and the thicker (2–3 m) dykes near the thinner dykes show no such variation. The thinner (<15 cm) dykes also intrude pre-existing dykes (Fig. 9d), and this may indicate the polygenetic nature of the DLIP eruption (Sheth & Cañón-Tapia 2015). There must have been considerable temporal separation between each intrusion episode, because the local stress field due to intrusion has a maximum horizontal stress orientation (SH_{max}) perpendicular to the dykes (Gudmundsson 2011). As there is a dilation component perpendicular to dyke intrusion, the stress fields are not compatible.

(6) Fault-offset dykes: some of the dykes are faulted, i.e. they are displaced along faults/brittle shears (Fig. 10). The approximately E–W-trending (Fig. 10a) and approximately N–S-trending (Fig. 10b) dykes both exhibit slip that is mostly sinistral and rarely dextral. These are the group I dykes of Hooper *et al.* (2010), and are all <30 cm thick. More than ten faulted dykes were identified at Korlai, Borlai and Barashiv (locations in Figs 2 & 3); these dykes do not have a preferred trend (Fig. 3e) and date from *c.* 66–65 Ma, i.e. predate the WDSZ deformation (Hooper *et al.* 2010). Offset dykes may often be confused with dykes that follow anisotropies (Figs 1d, 7a–d & 9a, b). However, the obvious

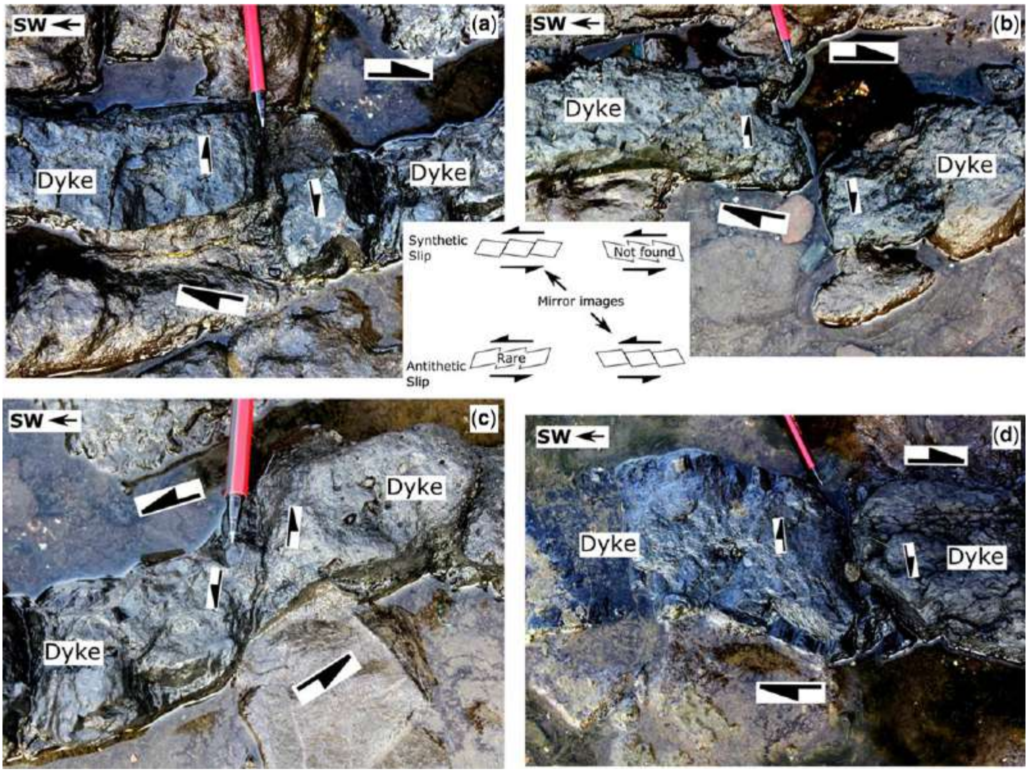

Fig. 11. Sub-horizontal outcrops showing possible 'shear-band' and 'domino-type' boudins at Murud (Figs 2 & 3 show locations). (**a**, **c**) Possible domino-type boudins; (**b**, **d**) possible shear-band boudins. (b, d) show drag along the shear. The small half-arrows show the sense of shear in the dyke blocks and the larger, half-arrows show the bulk shear sense. Inset: synthetic and antithetic shear-band and domino boudins (modified from Goscombe & Passchier 2003, fig. 1).

difference is the thickness of dykes following anisotropies. In fault-offset dykes, dyke lithologies are not observable along the anisotropy due to brittle failure, which does not allow smearing along the fault/brittle shear plane. This is because dykes cool and become brittle comparatively quickly (over a few days to a few months). However, tectonic deformation occurs over a very long time span (>1 Ma), so therefore dykes always deform in the brittle domain. Thickness often remains almost uniform along the length of dykes when they intrude along anisotropies.

(7) Boudinaged dykes: the NW-trending *c.* 6 cm thick dykes at Murud and one N-trending *c.* 5 cm thick dyke at Borlai (location in Figs 2 & 3) are sheared, but the shears do not continue into the host rock (Figs 11 & 12a, b). In contrast, the faults/shears in (6) extend into the host rock, which means that these sheared dykes are either shear-band/synthetic/S-type or domino-type/antithetic/A-type boudins (Goscombe *et al.* 2004 and references therein). As there are no layers in the country rock, no scar/neck/passive folds developed near the inter-boudin space or along brittle shear planes. Shear-band boudins have synthetic drag on a curved inter-boudin surface, large slip and no dilation along the shear (Fig. 11a, c) (Etchecopar 1977; Goscombe & Passchier 2003; Pamplona & Rodrigues 2011), and some are prominently drag folded near fault planes (Fig. 11b, d). Domino-type boudins have straight, sharp inter-boudin surfaces, relatively small slip and no drag along the shear (Figs 11a & 12a) (Swanson 1992; Goscombe & Passchier 2003; Pamplona & Rodrigues 2011). The implication of these dykes being shear-band or domino-type boudinaged is that the dykes sheared sub-parallel to their approximately NE trends, which is indicated by their bulk shear sense (Fig. 11a–d). This interpretation

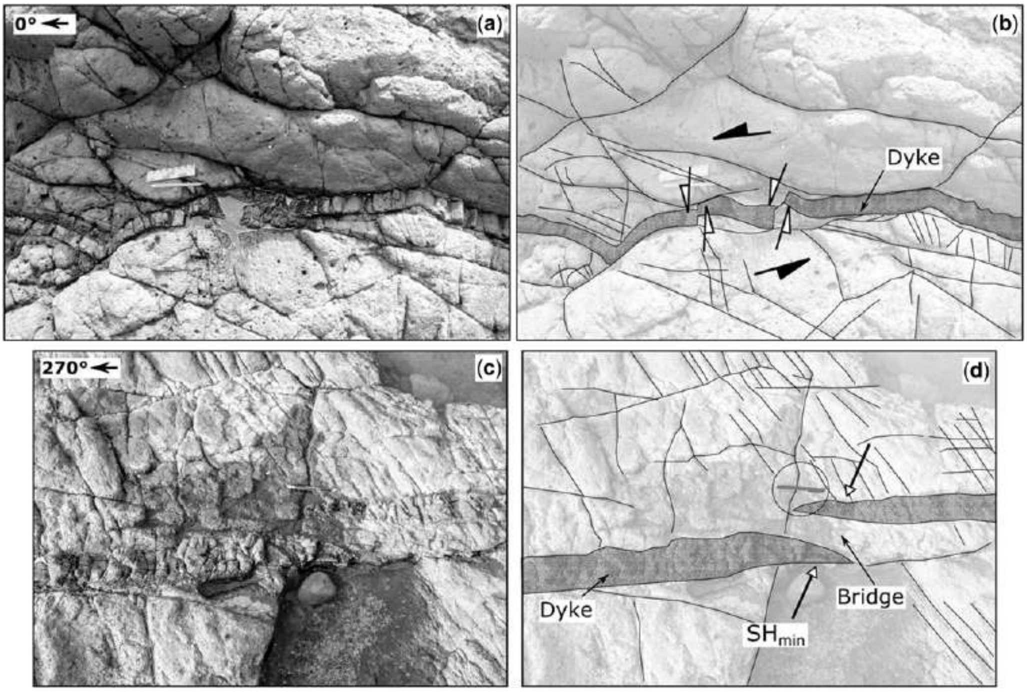

Fig. 12. (**a**, **b**) Dyke deformed into domino boudins at a sub-horizontal outcrop at Borlai (Figs 2 & 3 show locations). The smaller blank half arrows show the sense of shear in the dyke blocks and the larger half arrows show bulk shear sense. The 15 cm scale acts as a marker. (**c**, **d**) Host rock bridge between continuous dyke segments at a sub-horizontal outcrop at Barashiv (Figs 2 & 3 show locations). SH_{min}: minimum horizontal compression (i.e. extension) direction. Approximate NW extension may be indicated by the bridge. The 13 cm pen acts as a marker.

matches the dominant approximately N–S-trending and some approximately NE/NW-trending fault planes and shear senses reported by Misra *et al.* (2014) over a larger terrain, where structures other than boudins were also found. These dykes sheared either sinistrally (Figs 11a, b, d & 12a) or dextrally (Fig. 11c), with sinistral shear more prevalent. Some of the boudins are not associated with drag (Figs 11a & 12a) and some are strongly dragged (Fig. 11b). In places, the fault planes are subvertical and trend approximately NNW–SSE (Fig. 11a), but elsewhere they are synthetic (Fig. 11b, d) to the bulk shear sense. The sheared dyke at Borlai (Fig. 12a, b; location at Figs 2 & 3) intrudes a Y-plane and is sheared where sigmoid P-planes are observed. The dyke occupies a Y-plane and was itself sheared, which indicates that deformation continued over a substantial period of time.

(8) Rock bridges in dykes: continuous dyke segments are offset to form rock bridges (e.g. Hoek 1991; Almeida *et al.* 2013; Martínez-Poza *et al.* 2014). The centimetre-scale offsets at Barashiv (location in Fig. 2) are not fault-related. Rock bridges indicate coeval tectonics and magmatism, and hence are syntectonic intrusions (interpretation per Almeida *et al.* 2013; Martínez-Poza *et al.* 2014). They are present in only a few of the dykes (of <10 cm thickness) (Fig. 12c, d). In an overlap/bridge region ('overlap' is a near synonym of 'bridge') dykes curve and taper (Jerram & Petford 2012), and this is also seen in Figure 12c and d. Bridges indicate that flow fingers developed ahead of the bulk magma/lava flow (Jerram & Petford 2012, fig. 6.6a). The direction of minimum horizontal compression (SH_{min}) is shown to be perpendicular to the trend of the rock bridge. Faulted dykes can also be considered to be flanking structures where the fault planes are cross-cutting elements and the dykes host fabric elements (Passchier 2001; Mukherjee & Koyi 2009; Mukherjee 2014*b*). These flanking structures may be classified as normal drag, A type (Figs 10a–d & 12a, b), or normal drag, shear-band type (Fig. 11a–d). All may be considered to be type 1.2 flanking structures as per Mukherjee (2014*b*, fig. 18).

(9) Grooves on dyke margins: wall–magma interaction structures (Correa-Gomes *et al.* 2001) have been documented (Fig. 13; Misra 2015) at the chilled margins of >3 m thick dykes at Kharghar and Karnala (locations in Fig. 2). Early forming crystals in dykes tend to scratch the dyke itself, producing lineations or grooves, and these primary structures indicate syn-/post-tectonic dyking (Correa-Gomes *et al.* 2001). The grooves are sometimes tapered (Fig. 13a, b), and the tapered end indicates melt flow direction. Thus Figure 13b shows melt propagation from south towards north.

Approximately 60 km south of Mumbai, in the *c.* 40 km stretch of rocky beach, Korlai, Borlai, Barashiv and Murud (Fig. 2 shows locations) contain dykes. The other study locations, e.g. Kashid, Janjira and Nandgaon, do not contain dykes, although dykes do occur between the northernmost Korlai and southernmost Murud locations. Most of the dykes intrude brittle shears or are parallel to them (Fig. 14a, b), and thus appear to be the type (ii) dykes mentioned earlier. There are, however, excellent examples of brittle shears that are close to dykes yet are unrelated to them (Fig. 14c, d), and there are bulbous- to lensoid-shaped intrusive features near the dykes at Murud. The long axes of these intrusive features at the sub-horizontal outcrop trend approximately NNE (also Hooper *et al.* 2010). Tectonomagmatic fabrics such as grooves (Fig. 13a, b) were not observed in the vertical sections, possibly due to vegetation cover and/or erosion of the baked zones of the dykes. Foliation within the host rock is rare in the study area, and thus drag along the dyke margin could not be seen, unlike in Sengupta's (1983, 1995) work.

Determining the relative timing of the dykes from our field observations is problematic because cross-cutting relationships between dykes with approximately N–S and E–W trends and those with other trends are not easily observed. Hooper *et al.* (2010) identified approximately N–S-trending dykes cross-cutting approximately E–W-trending dykes at Borlai. We observed cross-cutting only at Borlai (Fig. 15a; location at Fig. 2), where *c.* 3 m thick dykes cross-cut an approximately NE-trending thick dyke, and in turn these all cross-cut approximately E–W-trending dykes (Hooper *et al.* 2010). Dyke thickness in the study area varies considerably (3 cm to >3 m) (Fig. 15b), although most of the dykes are <10 cm thick and only three are 2–3 m thick. As mentioned earlier, the thinner dykes appear to intrude pre-existing fractures of varying trends, but at outcrop scale the >300 cm thick

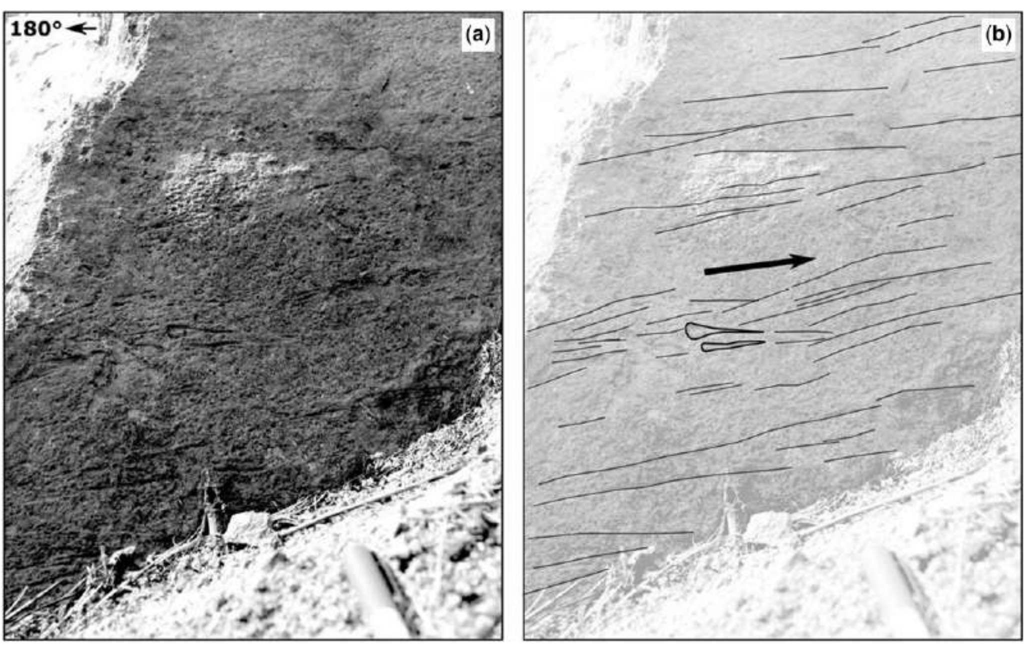

Fig. 13. Part of a chilled margin (**a**) and line drawing (**b**) of an approximately N–S-trending dyke at a subvertical outcrop at Kharghar Hills (Figs 2 & 3 show locations). The elongated grooves (thin lines) indicate flow of magma through a fault, and the tapered ones (arrows) show flow direction, marked by a bold arrow, towards the pointed end of the groove. The flow of magma was towards north in this case. The pen in the foreground acts as a marker.

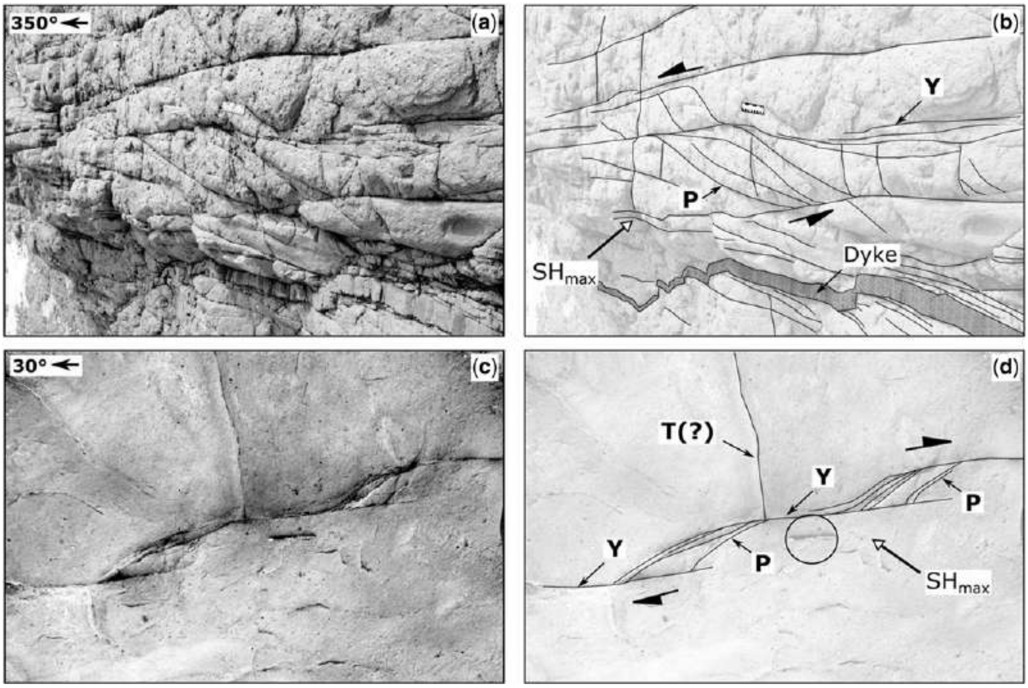

Fig. 14. Excellent examples of brittle shears at sub-horizontal outcrops (**a**, **b**) at Borlai. Note the parallel dyke to the west (below) of the brittle shear. The 15 cm scale acts as a marker; (**c**, **d**) brittle shear with conspicuous mineralized P- and Y-planes at Korlai. SH_{max}: maximum horizontal compression direction. The 13 cm pen acts as a marker. See Figures 2 and 3 for locations.

dykes appear not to. There are about five 10–30 cm thick dykes with bridges, and more than ten 30–100 cm thick dykes with branches or apophyses. The formation of these geometric features is most possibly related to tectonomagmatic factors, but this requires further study.

Discussion

We studied dyke outcrops in the WDSZ to understand their relationships with brittle shears/faults. To study dyke–shear relationships in more detail, one could also look at dyke rock under an optical microscope and investigate mineral preferred orientations, as carried out by Smith *et al.* (1993). Dykes intruding brittle shears/faults have also been identified on remote sensing images, e.g. Isola *et al.* (2014) in the East African Rift System and Misra *et al.* (2014) in the present study area. Scale of observation is important. At a regional scale, deformation can be identified on remote sensing images, and thus P-/R-shears along dyke margins, apophyses/branches/horns, grooves on baked margins, and boudins, etc. may not be seen. Dykes occupying P-/Y-planes, fault-offset dykes, m-scale rock bridges, etc. may be identified at a meso-scale. At a micro-scale, grain orientations, very small faults/brittle shears, and deformation bands in the host rock and dykes, etc. may be identified to indicate local-scale relationships. Regional- to local-scale deformation may yield structures with similar trends.

We report detailed relationships between dykes and brittle shears/faults where they are best observed, i.e. at sub-horizontal outcrops. Such outcrops in the WDSZ typically occur along wave-cut platforms or rocky beaches along the coast. Dykes were also observed at subvertical exposures along road-cut exposures. However, here the WDSZ is densely vegetated, especially during the rainy season, and most of the time thick soil horizons are formed, so identifying subtle features, e.g. grooves (Fig. 13), is relatively difficult. On the other hand, due to the complete lack of vegetation on the rocky beaches and wave-cut platforms, subtle structures (such as those in Figs 4–6, 12 & 14) here are easily seen.

We noted that some dykes were faulted, such as those at Korlai, Borlai and Barashiv (Fig. 10), and others were sheared, such as those at Murud (Figs 11 & 12a). At all these locations these group I

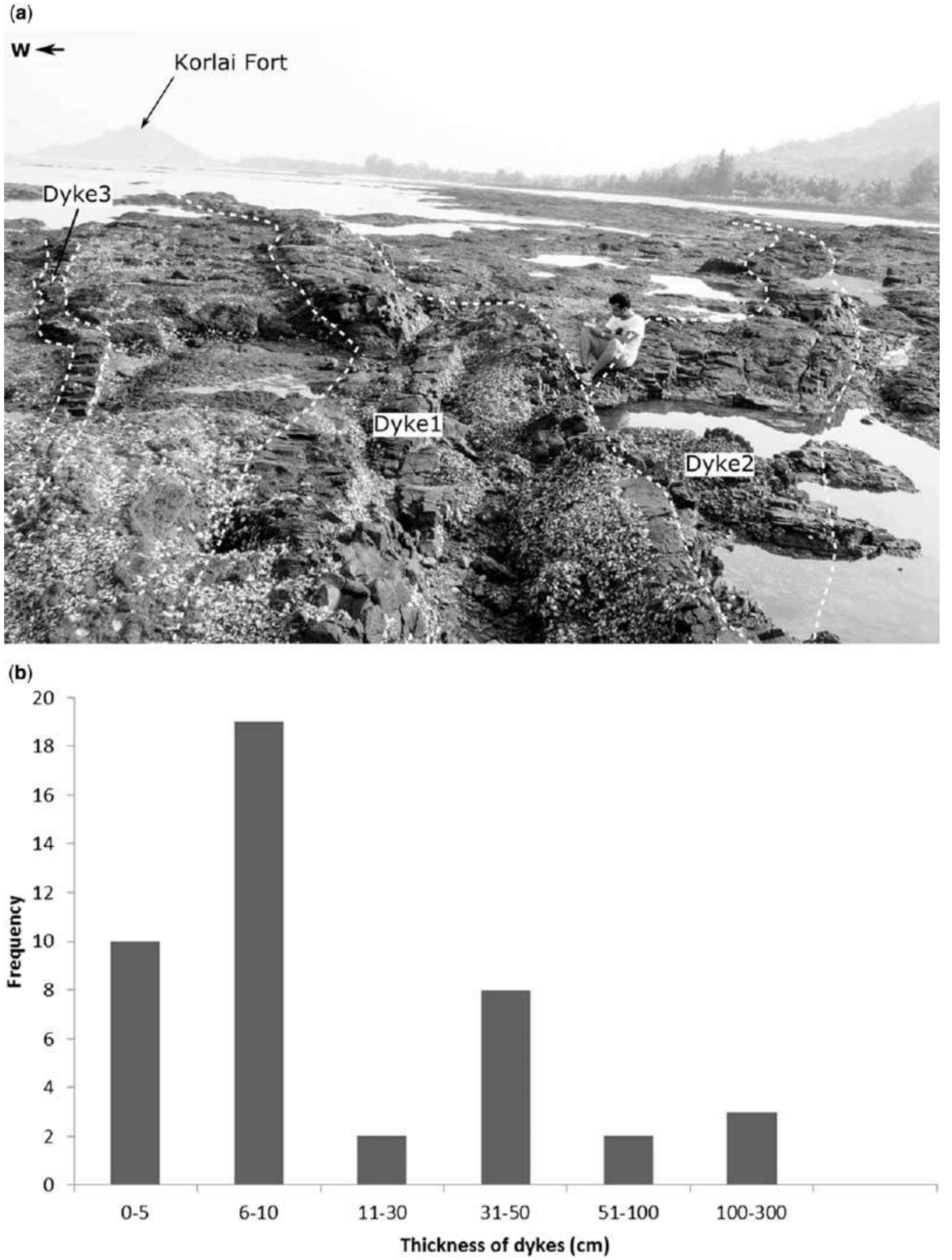

Fig. 15. (**a**) Cross-cut relation between dykes at Borlai (Figs 2 and 3 for locations). The location Korlai can be seen towards N at some distance. Around 2–3 m thick Dyke 1 with *c*. N trend cross-cuts *c*. NE trending *c*. 2–3 m Dyke 2. The former dyke is clearly younger. Dyke 3 is another *c*. N–S trending *c*. 30 cm thick dyke without a cross-cutting relation with any of the dykes. These dyke names do not correspond to Group I, II and III dykes of Hooper *et al.* (2010). Sandipan Saha makes notes while acting as a marker. (**b**) Histogram showing number of dykes as frequency in vertical axis, for corresponding thickness ranges along the horizontal axis.

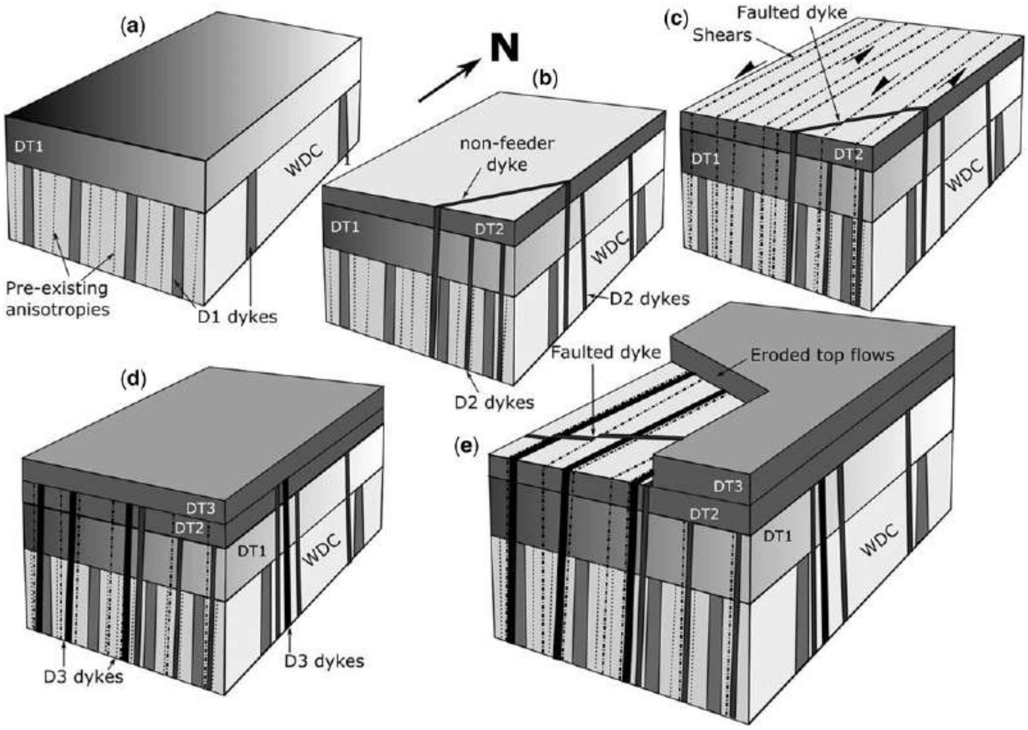

Fig. 16. Preferred tectonic model explaining the deformation in the study area (**a**–**e**) progressively advancing in time, which is detailed in the 'Discussion'. WDC: Western Dharwar Craton; DT1: first group of flows of the Deccan Traps (possibly of Kalsubai and Lonavala subgroups); DT2: second group of flows (possibly of the Karla, Elephanta and Diveghat Formations); DT3: third group of flows (possibly of the Purandargarh and Mahabaleshwar formations); D1, D2 and D3: stages of feeder dykes corresponding to the DT1, DT2 and DT3 flows, respectively. These dyke names do not correspond to group I, II and III dykes of Hooper *et al.* (2010). One non-feeder is shown in (b), which is faulted in the next stage (c) due to intensified shearing. Event chart in Table 2 supports this. The groups mentioned in Figure 16 are for flows corresponding to dyke 'names' DT1 etc.

dykes of Hooper *et al.* (2010) are non-oriented and trend approximately NNW, NE and WSW (Fig. 3e). Such dykes were emplaced prior to deformation of the basaltic flows in the study area, i.e. these dykes are pre-tectonic. The flows belong to the Karla, Elephanta and Diveghat lithostratigraphic Formations. There may be older formations below the exposed formations, hosting dykes related to these flows.

In addition to the group I dykes, we also studied numerous other dykes that either had brittle shear planes along their margins or were emplaced along pre-existing brittle shears and fractures. These are the group II and III dykes of Hooper *et al.* (2010). However, we were unable to differentiate between these two groups, since they are separated by the geochronologic dates of the dyke rocks. The 'absolute' ages of the dykes are not relevant to this study, and their relative ages are more important, so we have simply separated group I from group II and III dykes based on our field evidence. The group I dykes are older than the group II and III dykes. Dessai & Bertrand (1995) also reported one such group II/III dyke that was emplaced within an approximately N-trending fault plane. We observed P-planes along the boundaries of the dykes (groups II and III), which might indicate syn-tectonic intrusion. All the dykes intruding into brittle shears or faults (i.e. groups II and III) show sinistral kinematics. Only one faulted group I dyke is dextral sheared. Out of the *c.* 100 faults and brittle shears, only three show dextral kinematics.

T-planes passing through both the dykes and the host rock indicate that deformation also continued after magmatism. Cross-joints also indicate post-magmatic deformation. When cross-joints are present in the host rock as well as in the dyke, they may be related to tectonic deformation. When cross-/transverse joints are present only in dykes and are near orthogonal to each other, they are most likely related to dyke cooling (see Budkewitsch & Robin 1994; Gudmundsson 2011). Longitudinal joints (Fig. 4a, b) are commonly observed in dykes of various thicknesses (3 cm to >300 m), and do not act as Y-planes, i.e. there are no sigmoid P-planes associated with them. Dykes along the P- and Y-planes provide some of the best evidence of post-tectonic magmatism. Grooves in the baked zones of dykes also reliably indicate post-deformation intrusion. These dykes have strong, approximately N–S, NE or NW, trends, which match the brittle shear Y-plane trends (Fig. 3e). Most of the dykes, 33 of the 43 studied here, can be identified as group II/III. Cross-cutting relationships (Fig. 15) show that approximately N-trending dykes define the last intrusion event in the WDSZ coastal area. This may be related to the final stages of India–Seychelles separation at *c.* 63–62 Ma. Deformation continued after intrusion, which faulted or sheared the dykes. These faults/shears resemble reactivated faults because intrusion-related deformation is tectonically modified (Holdsworth *et al.* 1997 for details). Such dykes can reveal regional palaeostress tensors for tectonic deformation following dyke intrusion (Lisle 1989).

All the dykes in the present study area belong to the Ambenali and Mahabaleshwar chemostratigraphic Formations, which together correspond approximately to the Purandargarh and Mahabaleshwar lithostratigraphic Formations (Table 1). Thus they are all younger than the host rocks and could have been feeders to younger flows that have possibly been eroded.

Figure 16 summarizes our understanding of the deformation and dyking history based on the present study and literature review. The first flows of the Deccan Traps, possibly belonging to the Kalsubai and Lonavala subgroups, were emplaced on top of the *c.* 2.5 Ga Western Dharwar Craton (WDC). The pre-existing anisotropies of the WDC possibly guided magma to feed the oldest flows (DT1 in Fig. 16a), although not all dykes would have followed pre-existing fabrics. The fabrics, which are not inherited, are not optimally oriented to the tectonomagmatic stress. The WDC would have hosted most of the oldest dykes (D1 dykes in Fig. 16a) of the Deccan Traps in the WDSZ. Deformation related to rifting between *c.* 70 and 65 Ma might also have begun by this time, but this is difficult to ascertain due to the paucity of evidence. In the second stage (Fig. 16b), further layers of the Deccan Traps (DT2 in Fig. 16a) were emplaced, possibly the Karla, Elephanta and Diveghat Formations. It

Table 2. *Event chart for observations made during this study and literature review*

Event	Description	Observations
Coastal WDSZ, DT3	Third phase of Deccan flow: Purandargarh and Mahabaleshwar Formations	DT3 is fed by D3 dykes; D3 dykes occupy shears/faults, and D2 dykes are faulted/sheared
	Erosion of DT3 in coastal areas	
Peak Rifting	Intense brittle shear	All flows including some dykes are sheared
DT2	Second phase of Deccan flows: Karla, Elephanta and Diveghat Formations	DT2 is fed by D2 dykes; D3 dykes intrude within DT2 along a preferential approximately N–NNW trend; other trends are present
DT1	Earliest Deccan flows: Kalsubai and Lonavala subgroups	DT1 is emplaced and fed by D1 dykes; D2 dykes intrude within DT1 along a preferential approximately N–NNW trend; other trends are present
Western Dharwar Craton	Archean cratonic crust with pre-existing approximately N–NNW-trending metamorphic foliation, faults, shears, and dykes, etc. as weak anisotropies	D1 dykes intrude with a preferential, approximately N–NNW, trend; other trends are present

D1, D2 and D3: stages of feeder dyke corresponding to flows DT1, DT2 and DT3, respectively. These dyke names do not correspond to group I, II and III dykes of Hooper *et al.* (2010). The left side of the thick dotted line indicates eroded Deccan flows in the coastal areas of the WDSZ. This explains the presence of D3 dykes with no feeder attributes (e.g. Vanderkluysen *et al.* 2011). Figure 16 supports this chart.

is expected that feeder dykes for these flows were hosted by DT1 layers and the WDC. In the third stage (Fig. 16c), rift-related deformation intensified, leading to widespread faulting/brittle shearing of WDC, DT1 and DT2 layers along with several D1 and D2 dykes. It is expected that there are some of these dykes in the study area, and many of them may be beneath thick younger Deccan Trap flows (DT2 flows of the Karla, Elephanta and Diveghat Formations). In the fourth stage (Fig. 16d), further flows of the Deccan Traps (here, DT3) were emplaced on top of the DT2 flows. Most of the dykes feeding the DT3 flows occupied the pre-existing dominant approximately N-trending and some approximately NE–NW-trending shears/ faults. We have observed that most of the dykes are of this type, i.e. groups II and III of Hooper *et al.* (2010). Pre-existing structures such as faults/brittle shears were preferentially intruded because they were weaker than the host rock (Fig. 1a; reviews by Misra & Mukherjee 2015*b*). Rift-related deformation possibly continued at this time. This is implied by evidence of syn-deformation intrusion, which we have previously described. Dykes emplaced at high angle to the shears will have become faulted during progressive deformation, and those trending parallel to the shears may also have re-sheared and become boudinaged. In the final stage (Fig. 16e), close to present day, we do not observe DT3 flows/layers, i.e. those belonging to the Purandargarh and Mahabaleshwar Formations in the Korlai to Murud region. These were probably eroded, thus exposing the older Karla, Elephanta and Diveghat Formations of the DT2 flows, and these flows host the feeder dykes for younger formations. Finally, the top of the DT2 flows constitute the present day sub-horizontal outcrops.

Conclusions

This study highlighted key aspects in the deformation history of the DLIP in and around Mumbai, India. This region, the WDSZ, is a zone of intense brittle strike-slip, dominantly sinistral, shear related to the Seychelles–India separation at *c.* 63–62 Ma. The WDSZ is intruded by numerous dykes, which have dominant trends of approximately N–NE, NW, and very few E. We conclude the following about the dykes and their deformation:

(1) Most of the study area is not intruded by dykes, whereas a few locations, e.g. Korlai and Borlai, have tens of dykes.

(2) Regionally, dykes in the WDSZ have dominant trends of approximately N, with some approximately NE and NW. They vary widely in length, width and trend, even at outcrop scale.

(3) The faults and brittle shears cut across many dykes, approximately 10 of the 43 observed. Many more dykes (approximately 33 of the 43 observed) intrude fractures and faults/ brittle shears or indicate syn- to post-deformational intrusion.

(4) Dykes intruding pre-existing faults, indicated by grooves along the baked zones of two dykes, are also evident. Dykes occupying P- and Y-planes have been identified from satellite images. Regionally, several dykes in the WDSZ intrude brittle shears/fault planes.

(5) It is erroneous to interpret the Seychelles–India rifting as simple near-E–W extension at *c.* 63–62 Ma from the general approximately N–S trend of the dykes, and the extension direction must be calculated from faults or brittle shears. Such a study has been carried by Misra *et al.* (2014) for part of the WDSZ and may be used to study extension direction throughout the sheared margin.

IIT Bombay partially funded the fieldwork. Abhimanyu Maitra, Mainak Choudhuri and Sandipan Saha (Reliance Industries Limited) are thanked for accompanying AAM to one of the field locations and for their discussions. Abhimanyu Maitra is owed special thanks for sharing a few field photographs (Figs 5a, c, 6a & 7a, c). SM acknowledges the late Usha Chaterjee for spontaneously assisting in household activities and providing the free time to do research. Angharad Hills, Phil Leat, Rachael Kriefman and Tamzin Anderson (Geological Society, London) are acknowledged for their support. We also thank the two anonymous reviewers for their critical comments, and the anonymous handling editor for assistance. The abstract Misra & Mukherjee (2015*b*) encapsulates this work. AAM and SM conducted fieldwork. AAM primarily wrote the draft, and the paper was finalized by both AAM and SM.

References

Abdelmalak, M.M., Mourgues, R., Galland, O. & Bureau, D. 2012. Fracture mode analysis and related surface deformation during dyke intrusion: results from 2D experimental modelling. *Earth and Planetary Science Letters*, **359**, 93–105.

Agashe, L.V. & Gupte, R.B. 1972. Mode of eruption of Deccan Trap Basalts. *Bulletin of Volcanology*, **25**, 591–601.

Almeida, J., Dios, F., Mohriak, W.U., Valeriano, C.D.M., Heilbron, M., Eirado, L.G. & Tomazzoli, E. 2013. Pre-rift tectonic scenario of the Eo-Cretaceous Gondwana break-up along SE Brazil–SW Africa: insights from tholeiitic mafic dyke swarms. *In*: Mohriak, W.U., Danforth, A., Post, P.J., Brown, D.E., Tari, G.C., Nemčok, M. & Sinha, S.T. (eds) *Conjugate Divergent Margins*. Geological Society, London, Special Publications, **369**, 11–40.

Anderson, E.M. 1951. *The Dynamics of Faulting and Dyke Formation with Special Applications to Britain*. 2nd edn. Oliver and Boyd, Edinburgh.

AUBOURG, C., GIORDANO, G., MATTEI, M. & SPERANZA, F. 2002. Magma flow in sub-aqueous rhyolitic dikes inferred from magnetic fabric analysis (Ponza Island, W. Italy). *Physics and Chemistry of the Earth, Parts A/B/C*, **27**, 1263–1272.

AUDEN, J.B. 1949. Dykes in western India: a discussion of their relationships with the Deccan Trap. *Transaction of the National Institute of Sciences in India*, **3**, 13–157.

BEANE, J.E., TURNER, C.A., HOOPER, P.R., SUBBARAO, K.V. & WALSH, J.N. 1986. Stratigraphy, composition and form of the Deccan basalts, Western Ghats, India. *Bulletin of Volcanology*, **48**, 61–83.

BHATTACHARJI, S., CHATTERJEE, N., WAMPLER, J.M., NAYAK, P.N. & DESHMUKH, S.S. 1996. Indian intraplate and continental margin rifting, lithospheric extension, and mantle upwelling in Deccan flood basalt volcanism near the K/T boundary: evidence from mafic dike swarms. *The Journal of Geology*, **104**, 379–398.

BHATTACHARYA, G.C. & YATHEESH, V. 2015. Plate-tectonic evolution of the deep ocean basins adjoining the Western Continental Margin of India – a proposed model for the early opening scenario. *In*: MUKHERJEE, S. (ed.) *Petroleum Geosciences: Indian Contexts*. Springer, Cham, 1–61.

BLYTH, F.G. 1949. The sheared porphyrite dykes of South Galloway. *Quarterly Journal of the Geological Society*, **105**, 393–423.

BLEEKER, W. & ERNST, R. 2006. Short-lived mantle generated magmatic events and their dyke swarms: the key unlocking Earth's paleogeographic record back to 2.6 Ga. *In*: HANSKI, E., MERTANEN, S., RÄMÖ, T. & VUOLLO, J. (eds) *Dyke Swarms-Time Markers of Crustal Evolution: Selected Papers of the Fifth International Dyke Conference in Finland*, 31 July–3 Aug 2005, Rovaniemi, Finland.

BONDRE, N.R., HART, W.K. & SHETH, H.C. 2006. Geology and geochemistry of the Sangamner Mafic Dike Swarm, Western Deccan Volcanic Province, India: implications for regional stratigraphy. *The Journal of Geology*, **114**, 155–170.

BUDKEWITSCH, P. & ROBIN, P.Y. 1994. Modelling the evolution of columnar joints. *Journal of Volcanology and Geothermal Research*, **59**, 219–239.

CADMAN, A.C., HARRIS, D. & RYAN, B. 1993. *An investigation of some metamorphosed mafic dykes of the Nain area, Labrador, Part 1*. Current Research. Geological Survey Branch, Newfoundland Department of Mines and Energy, Report, 93-1.

CATER, F.W. 1982. Intrusive rocks of the Holden and Lucerne Quadrangle, Washington – the relation of depth zones, composition, textures and emplacement of plutons. *Geological Survey Professional Paper*, **1220**, 86.

CHANDRASEKHARAM, D. 2003. Deccan flood basalts. *In*: MAHADEVAN, T.M., ARORA, B.R. & GUPTA, K.R. (eds) *Indian Continental Lithospehre: Emerging Research Trends*. Memoir Geological Society of India, Bangalore, **53**, 197–214.

CHENET, A.L., QUIDELLEUR, X., FLUTEAU, F., COURTILLOT, V. & BAJPAI, S. 2007. ^{40}K–^{40}Ar dating of the Main Deccan large igneous province: further evidence of KTB age and short duration. *Earth and Planetary Science Letters*, **263**, 1–15.

CLEMENTE, C.S., AMORÓS, E.B. & CRESPO, M.G. 2007. Dike intrusion under shear stress: effects on magnetic and vesicle fabrics in dikes from rift zones of Tenerife (Canary Islands). *Journal of Structural Geology*, **29**, 1931–1942.

COLLIER, J.S., SANSOM, V., ISHIZUKA, O., TAYLOR, R.N., MINSHULL, T.A. & WHITMARSH, R.B. 2008. Age of Seychelles–India break-up. *Earth and Planetary Science Letters*, **272**, 264–277.

CORREA-GOMES, L.C., SOUZA FILHO, C.R., MARTINS, C.J.F.N. & OLIVEIRA, E.P. 2001. Development of symmetrical and asymmetrical fabrics in sheet-like igneous bodies: the role of magma flow and wall-rock displacements in theoretical and natural cases. *Journal of Structural Geology*, **23**, 1415–1428.

CREIXELL, C., PARADA, M.Á., ROPERCH, P., MORATA, D., ARRIAGADA, C. & DE ARCE, C.P. 2006. Syntectonic emplacement of the Middle Jurassic Concón Mafic Dike Swarm, Coastal Range, central Chile (33° S). *Tectonophysics*, **425**, 101–122.

DANIELS, K.A., KAVANAGH, J.L., MENAND, T. & STEPHEN, J.S.R. 2012. The shapes of dikes: evidence for the influence of cooling and inelastic deformation. *Geological Society of America Bulletin*, **124**, 1102–1112.

DAVIS, G.H., BUMP, A.P., GARCÍA, P.E. & AHLGREN, S.G. 2000. Conjugate Riedel deformation band shear zones. *Journal of Structural Geology*, **22**, 169–190.

DESHMUKH, S.S. & SEHGAL, M.N. 1988. Mafic dyke swarms in Deccan Volcanic Province of Madhya Pradesh and Maharashtra. *Geological Society of India, Memoir*, **10**, 323–340.

DESHPANDE, G.G. 1998. *Geology of Maharashtra*. Geological Society of India, Bangalore, 129–162.

DESSAI, A. & BERTRAND, H. 1995. The 'Panvel flexure' along the western Indian continental margin: an extensional fault structure related to Deccan magmatism. *Tectonophysics*, **241**, 165–178.

DESSAI, A.G. & VIEGAS, A. 2010. Petrogenesis of alkaline rocks from Murud-Janjira, in the Deccan Traps, Western India. *Mineralogy and Petrology*, **98**, 297–311.

ETCHECOPAR, A. 1977. A plane kinematic model of progressive deformation in a polycrystalline aggregate. *Tectonophysics*, **39**, 121–139.

FÉMÉNIAS, O., DIOT, H., BERZA, T., GAUFFRIAU, A. & DEMAIFFE, D. 2004. Asymmetrical to symmetrical magnetic fabric of dikes: paleo-flow orientations and paleo-stresses recorded on feeder-bodies from the Motru Dike Swarm (Romania). *Journal of Structural Geology*, **26**, 1401–1418.

FIALKO, Y.A. & RUBIN, A.M. 1999. Thermal and mechanical aspects of magma emplacement in giant dike swarms. *Journal of Geophysical Research: Solid Earth*, **104**, 23033–23049.

FOSSEN, H. 2016. *Structural Geology*. 2nd edn. Cambridge University Press.

GAFFNEY, E.S., DAMJANAC, B. & VALENTINE, G.A. 2007. Localization of volcanic activity: 2. Effects of pre-existing structure. *Earth and Planetary Science Letters*, **263**, 323–338.

GALLAND, O., BURCHARDT, S., HALLOT, E., MOURGUES, R. & BULOIS, C. 2014. Dynamics of dikes versus cone sheets in volcanic systems. *Journal of Geophysical Research: Solid Earth*, **119**, 6178–6192.

GESHI, N., KUSUMOTO, S. & GUDMUNDSSON, A. 2010. Geometric difference between non-feeder and feeder dikes. *Geology*, **38**, 195–198.

GLAZNER, A.F., BARTLEY, J.M. & CARL, B.S. 1999. Oblique opening and noncoaxial emplacement of the Jurassic independence dike swarm, California. *Journal of Structural Geology*, **21**, 1275–1283.

GODBOLE, S., RANA, R. & NATU, S. 1996. Lava stratigraphy of Deccan basalts of western Maharashtra. *Gondwana Geological Magazine, Special Publication*, **2**, 125–134.

GOSCOMBE, B.D. & PASSCHIER, C.W. 2003. Asymmetric boudins as shear sense indicators – an assessment from field data. *Journal of Structural Geology*, **25**, 575–589.

GOSCOMBE, B.D., PASSCHIER, C.W. & HAND, M. 2004. Boudinage classification: end-member boudin types and modified boudin structures. *Journal of Structural Geology*, **26**, 739–763.

GROVES, D.I., KORKIAKOSKI, E.A., MCNAUGHTON, N.J., LESHER, C.M. & COWDEN, A. 1986. Thermal erosion by komatiites at Kambalda, Western Australia and the genesis of nickel ores. *Nature*, **319**, 136–139.

GUDMUNDSSON, A. 1984. Formation of dykes, feeder-dykes, and the intrusion of dykes from magma chambers. *Bulletin Volcanologique*, **47**, 537–550.

GUDMUNDSSON, A. 2002. Emplacement and arrest of sheets and dykes in central volcanoes. *Journal of Volcanology and Geothermal Research*, **116**, 279–298.

GUDMUNDSSON, A. 2003. Surface stresses associated with arrested dykes in rift zones. *Bulletin of Volcanology*, **65**, 606–619.

GUDMUNDSSON, A. 2006. How local stresses control magma-chamber ruptures, dyke injections, and eruptions in composite volcanoes. *Earth-Science Reviews*, **79**, 1–31.

GUDMUNDSSON, A. 2011. *Rock Fractures in Geological Processes*. Cambridge University Press, New York.

GUDMUNDSSON, A. & LOETVEIT, I.F. 2005. Dyke emplacement in a layered and faulted rift zone. *Journal of Volcanology and Geothermal Research*, **144**, 311–327.

HAMLING, I.J., AYELE, A. *ET AL.* 2009. Geodetic observations of the ongoing Dabbahu rifting episode: new dyke intrusions in 2006 and 2007. *Geophysical Journal International*, **178**, 989–1003.

HANSKI, E., MERTANEN, S., RÄMÖ, T. & VUOLLO, J. (eds) 2006. *Dyke Swarms-Time Markers of Crustal Evolution: Selected Papers of the Fifth International Dyke Conference in Finland*, 31 July–3 Aug 2005, Rovaniemi, Finland.

HEAMAN, L.M. & TARNEY, J. 1989. U Pb baddeleyite ages for the Scourie dyke swarm, Scotland: evidence for two distinct intrusion events. *Nature*, **340**, 705–708.

HODGE, K.F., CARAZZO, G. & JELLINEK, A.M. 2012. Experimental constraints on the deformation and breakup of injected magma. *Earth and Planetary Science Letters*, **325**, 52–62.

HOEK, J.D. 1991. A classification of dyke-fracture geometry with examples from Precambrian dyke swarms in the Vestfold Hills, Antarctica. *Geologische Rundschau*, **80**, 233–248.

HOLDSWORTH, R.E., BUTLER, C.A. & ROBERTS, A.M. 1997. The recognition of reactivation during continental deformation. *Journal of the Geological Society*, **154**, 73–78.

HOOPER, P., WIDDOWSON, M. & KELLEY, S. 2010. Tectonic setting and timing of the final Deccan flood basalt eruptions. *Geology*, **38**, 839–842.

HOU, G. 2012. Mechanism for three types of mafic dyke swarms. *Geoscience Frontiers*, **3**, 217–223.

HUTTON, D. 1992. Granite sheeted complexes: evidence for the dyking ascent mechanism. *Transactions of the Royal Society of Edinburgh, Earth Sciences*, **83**, 377–382.

ISOLA, I., MAZZARINI, F., BONINI, M. & CORTI, G. 2014. Spatial variability of volcanic features in early-stage rift settings: the case of the Tanzania Divergence, East African rift system. *Terra Nova*, **26**, 461–468.

JERRAM, D. & PETFORD, N. 2012. *The Field Description of Igneous Rocks. 2nd edn. The Geological Field Guide Series*. Wiley-Blackwell, West Sussex.

JU, W., HOU, G. & HARI, K. 2013. Mechanics of mafic dyke swarms in the Deccan large igneous province: palaeostress field modelling. *Journal of Geodynamics*, **66**, 79–91.

KATZ, Y., WEINBERGER, R. & AYDIN, A. 2004. Geometry and kinematic evolution of Riedel shear structures, Capitol Reef National Park, Utah. *Journal of Structural Geology*, **26**, 491–501.

KAVANAGH, J.L. & SPARKS, R.S.J. 2011. Insights of dyke emplacement mechanics from detailed 3D dyke thickness datasets. *Journal of the Geological Society, London*, **168**, 965–978.

KRAUS, S., POBLETE, F. & ARRIAGADA, C. 2010. Dike systems and their volcanic host rocks on King George Island, Antarctica: implications on the geodynamic history based on a multidisciplinary approach. *Tectonophysics*, **495**, 269–297.

LISLE, R.J. 1989. Paleostress analysis from sheared dike sets. *Geological Society of America Bulletin*, **101**, 968–972.

MARTÍNEZ-POZA, A.I., DRUGUET, E., CASTAÑO, L.M. & CARRERAS, J. 2014. Dyke intrusion into a pre-existing joint network: the Aiguablava lamprophyre dyke swarm (Catalan Coastal Ranges). *Tectonophysics*, **630**, 75–90.

MÈGE, D. & KORME, T. 2004. Dyke swarm emplacement in the Ethiopian Large Igneous Province: not only a matter of stress. *Journal of Volcanology and Geothermal Research*, **132**, 283–310.

MÉRIAUX, C. & LISTER, J.R. 2002. Calculation of dike trajectories from volcanic centers. *Journal of Geophysical Research: Solid Earth*, **107**, 2077.

MISRA, A.A. 2015. *Sheared Nature of the Indian Western Continental Margin around Mumbai, India: Onshore and Offshore Geoscientific Studies*. Unpublished PhD thesis, Indian Institute of Technology Bombay, India, 253.

MISRA, A.A. 2015. Photograph of the month. *Journal of Structural Geology*, **73**, iii.

MISRA, A.A. & MUKHERJEE, S. 2015*a*. Dyke-brittle shear relation in the western Deccan Traps near Mumbai, India. *Tectonic Studies Group Annual Meeting*, Edinburgh, January 2015. https://doi.org/10.13140/2.1.1788.1921

MISRA, A.A. & MUKHERJEE, S. 2015*b*. *Tectonic Inheritance in Continental Rifts and Passive Margins*. SpringerBriefs in Earth Sciences, Berlin.

Misra, A.A., Bhattacharya, G., Mukherjee, S. & Bose, N. 2014. Near N–S paleo-extension in the western Deccan region, India: does it link strike-slip tectonics with India–Seychelles rifting? *International Journal of Earth Sciences*, **103**, 1645–1680.

Misra, A.A., Sinha, N. & Mukherjee, S. 2015. Repeat ridge jumps and microcontinent separation: insights from NE Arabian Sea. *Marine and Petroleum Geology*, **59**, 406–428.

Misra, K.S. 2008. Dyke swarms and dykes within the Deccan Volcanic Province, India. *In*: Srivastava, R.K., Sivaji, C.h. & Chalapathi Rao, N.V. (eds) *Indian Dykes: Geochemistry, Geophysics and Geochemistry*. Narosa Publishing House, New Delhi, 57–72.

Mitchell, C. & Widdowson, M. 1991. A geological map of the southern Deccan Traps, India and its structural implications. *Journal of the Geological Society, London*, **148**, 495–505.

Mukherjee, S. 2011. Mineral fish: their morphological classification, usefulness as shear sense indicators and genesis. *International Journal of Earth Sciences*, **100**, 1303–1314.

Mukherjee, S. 2013*a*. *Deformation Microstructures in Rocks*. Springer, Heidelberg.

Mukherjee, S. 2013*b*. Higher Himalaya in the Bhagirathi section (NW Himalaya, India): its structures, backthrusts and extrusion mechanism by both channel flow and critical taper mechanisms. *International Journal of Earth Sciences*, **102**, 1851–1870.

Mukherjee, S. 2014*a*. *Atlas of Shear Zone Structures in Meso-scale*. Springer, Cham.

Mukherjee, S. 2014*b*. Review of flanking structures in meso-and micro-scales. *Geological Magazine*, **151**, 957–974.

Mukherjee, S. 2015. *Atlas of Structural Geology*. Elsevier, Amsterdam.

Mukherjee, S. & Koyi, H.A. 2009. Flanking microstructures. *Geological Magazine*, **146**, 517–526.

Mukherjee, S. & Koyi, H.A. 2010. Higher Himalayan Shear Zone, Sutlej section: structural geology and extrusion mechanism by various combinations of simple shear, pure shear and channel flow in shifting modes. *International Journal of Earth Sciences*, **99**, 1267–1303.

Opheim, J.A. & Gudmundsson, A. 1989. Formation and geometry of fractures, and related volcanism, of the Krafla fissure swarm, northeast Iceland. *Geological Society of America Bulletin*, **101**, 1608–1622.

Pamplona, J. & Rodrigues, B.C. 2011. Kinematic interpretation of shearband boudins: new parameters and ratios useful in HT simple shear zones. *Journal of Structural Geology*, **33**, 38–50.

Passchier, C.W. 2001. Flanking structures. *Journal of Structural Geology*, **23**, 951–962.

Passchier, C.W. & Trouw, R.A. 2005. *Microtectonics*. 2nd edn. Springer Verlag, Berlin.

Paquet, F., Dauteuil, O., Hallot, E. & Moreau, F. 2007. Tectonics and magma dynamics coupling in a dyke swarm of Iceland. *Journal of Structural Geology*, **29**, 1477–1493.

Perry, F.V., Valentine, G.A., Cogbill, A.H., Keating, G.N., Gaffney, E.S. & Damjanac, B. 2006. Control of basaltic feeder dike orientation by fault capture near Yucca Mountain, USA. *American Geophysical Union Fall Meeting*, San Francisco, 11–15 December 2006. 1, 0572, abstract V11B-0572.

Petit, J. 1987. Criteria for the sense of movement on fault surfaces in brittle rocks. *Journal of Structural Geology*, **9**, 597–608.

Philippon, M., Willingshofer, E., Sokoutis, D., Corti, G., Sani, F., Bonini, M. & Cloetingh, S. 2015. Slip re-orientation in oblique rifts. *Geology*, **43**, 147–150.

Rao, N.P., Roy, S. & Arora, K. 2013. Deep Scientific Drilling in Koyna, India – Brain-storming Workshop on Geological Investigations 19–20, March 2013. *Journal of the Geological Society of India*, **81**, 722–723.

Ray, R., Sheth, H.C. & Mallik, J. 2007. Structure and emplacement of the Nandurbar-Dhule mafic dyke swarm, Deccan Traps, and the tectonomagmatic evolution of flood basalts. *Bulletin of Volcanology*, **69**, 537–551.

Ray, R., Shukla, A.D. *et al.* 2008. Highly heterogeneous Precambrian basement under the central Deccan Traps, India: direct evidence from xenoliths in dykes. *Gondwana Research*, **13**, 375–385.

Reichardt, H. & Weinberg, R.F. 2012. The dike swarm of the Karakoram shear zone, Ladakh, NW India: linking granite source to batholith. *GSA Bulletin*, **124**, 89–103.

Renne, P.R., Sprain, C.J., Richards, M.A., Self, S., Vanderkluysen, L. & Pande, K. 2015. State shift in Deccan volcanism at the Cretaceous-Paleogene boundary, possibly induced by impact. *Science*, **350**, 76–78.

Rivalta, E., Taisne, B., Bunger, A. & Katz, R. 2015. A review of mechanical models of dike propagation: schools of thought, results and future directions. *Tectonophysics*, **638**, 1–42.

Roy, S., Rao, N.P., Akkiraju, V.V., Goswami, D., Sen, M., Bansal, B.K. & Nayak, S. 2013. Granitic basement below Deccan Traps Unearthed by drilling in the Koyna seismic zone, Western India. *Journal of the Geological Society of India*, **81**, 289–290.

Sengupta, S. 1983. Folding of boudinaged layers. *Journal of Structural Geology*, **5**, 197–210.

Sengupta, S. 1995. Patterns of foliation drag near walls of reoriented dykes. *Proceedings of the Indian Academy of Sciences – Earth and Planetary Sciences*, **104**, 433–446.

Sengupta, S. 1997. Contrasting fabrics in deformed dykes and host rocks: natural examples and a simplistic model. *In*: Sengupta, S. (ed.) *Evolution of GeologicalStructures in Micro- and Macro-Scales*. Chapman & Hall, London, 293–319.

Sheth, H.C. & Cañón-Tapia, E. 2015. Are flood basalt eruptions monogenetic or polygenetic? *International Journal of Earth Sciences*, **104**, 2147–2162.

Sheth, H.C., Zellmer, G.F., Demonterova, E.I., Ivanov, A.V., Kumar, R. & Patel, R.K. 2014. The Deccan tholeiite lavas and dykes of Ghatkopar–Powai area, Mumbai, Panvel flexure zone: geochemistry, stratigraphic status, and tectonic significance. *Journal of Asian Earth Sciences*, **84**, 69–82.

Smith, J.V., Miyake, Y. & Yamacuhi, S. 1993. Flow directions and groundmass shear zones in dykes, Shimane Peninsula, Japan. *Geological Magazine*, **130**, 117–120.

Srivastava, R. (ed.) 2011. *Dyke Swarms: Keys for Geodynamic Interpretation*. Springer, Berlin.

Swanson, M.T. 1992. Late Acadian-Alleghenian transpressional deformation: evidence from asymmetric boudinage in the Casco Bay area, coastal Maine. *Journal of Structural Geology*, **14**, 323–341.

Torres-Hernández, J.R., Labarthe-Hernández, G., Aguillón-Robles, A., Gómez-Anguiano, M. & Mata-Segura, J.L. 2006. The pyroclastic dikes of the Tertiary San Luis Potosí volcanic field: implications on the emplacement of Panalillo ignimbrite. *Geofísica Internacional*, **45**, 243–253.

Trippanera, D., Acocella, V., Ruch, J. & Abebe, B. 2015. Fault and graben growth along active magmatic divergent plate boundaries in Iceland and Ethiopia. *Tectonics*, **34**, 2318–2348.

Upadhyay, D., Kooijman, E., Singh, A.K., Mezger, K. & Berndt, J. 2015. The basement of the Deccan Traps and its Madagascar connection: constraints from xenoliths. *The Journal of Geology*, **123**, 295–307.

Vaidhyanadhan,, R. & Ramakrishnan, M. 2008. *Geology of India*. Geological Society of India Publication, Bangalore, **2**, 733–784.

Valdiya, K.S. 2011. Some burning questions remaining unanswered. *Journal of the Geological Society of India*, **78**, 299–320.

Valdiya, K.S. 2016. *The Making of India: Geodynamic Evolution*. Springer, 2nd edn.

Valentine, G.A. & Keating, G.N. 2007. Eruptive styles and inferences about plumbing systems at Hidden Cone and Little Black Peak scoria cone volcanoes (Nevada, USA). *Bulletin of Volcanology*, **70**, 105–113.

Valentine, G.A. & Krogh, K.E. 2006. Emplacement of shallow dikes and sills beneath a small basaltic volcanic center: the role of pre-existing structure (Paiute Ridge, southern Nevada, USA). *Earth and Planetary Science Letters*, **246**, 217–230.

Vanderkluysen, L., Mahoney, J.J., Hooper, P.R., Sheth, H.C. & Ray, R. 2011. The feeder system of the Deccan Traps (India): insights from dike geochemistry. *Journal of Petrology*, **52**, 315–343.

Watkeys, M.K. 2002. Development of the Lebombo rifted volcanic margin of southeast Africa. *In*: Menzies, M.A., Klemperer, S.L., Ebinger, C.J. & Baker, J. (eds) *Volcanic Rifted Margins*. Geological Society of America Special Paper, Boulder, **362**, 27–46.

Widdowson, M., Pringle, M. & Fernandez, O. 2000. A post K–T boundary (Early Palaeocene) age for Deccan-type feeder dykes, Goa, India. *Journal of Petrology*, **41**, 1177–1194.

Xu, S.-S., Nieto-Samaniego, A.F. & Alaniz-Alvarez, S.A. 2013. Emplacement of pyroclastic dykes in Riedel shear fractures: an example from the Sierra de San Miguelito, central Mexico. *Journal of Volcanology and Geothermal Research*, **250**, 1–8.

Ziv, A., Rubin, A.M. & Agnon, A. 2000. Stability of dike intrusion along preexisting fractures. *Journal of Geophysical Research*, **105**, 5947–5961.

Zulauf, G. & Helferich, S. 1997. Strain and strain rate in a synkinematic trondhjemitic dike: evidence for melt-induced strain softening during shearing (Bohemian Massif, Czech Republic). *Journal of Structural Geology*, **19**, 639–652.